

# Physics at Multi-TeV Linear Colliders

Timothy L. Barklow\*

*Stanford Linear Accelerator Center, Stanford University, Stanford, California 94309 USA*

Albert De Roeck†

*CERN, CH-1211, Geneva 23 Switzerland*

(Dated: December 18, 2001)

The physics at an  $e^+e^-$  linear collider with a center of mass energy of 3-5 TeV is reviewed. The following topics are covered: experimental environment, Higgs physics, supersymmetry, fermion pair-production,  $W^+W^-$  scattering, extra dimensions, non-commutative theories, and black hole production.

## I. INTRODUCTION

Presently planned  $e^+e^-$  linear collider (LC) projects will operate at an initial center of mass system (CMS) energy of about 500 GeV, with upgrades to higher energies designed in from the start. The TeV class colliders TESLA [1] and NLC/JLC [2, 3] target 800 GeV and 1-1.5 TeV, respectively, as their maximum CMS energies. Increasing the energy further would require either a change in acceleration technology or an extension in accelerator length beyond the presently foreseen 30-40 km [4]. This would also increase the number of active elements, which will likely decrease the overall efficiency of such a facility.

The nature of the new physics which will hopefully be discovered and studied at the LHC and a TeV class LC will determine the necessity and importance of exploring the multi-TeV range with a precision machine such as an  $e^+e^-$  collider. This paper summarizes the work of the E3 subgroup 2 on multi-TeV colliders of the Snowmass 2001 workshop ‘The Future of Particle Physics’.

Based on our knowledge today, the case for the multi-TeV collider rests on the following physics scenarios:

- The study of the Higgs

For a light Higgs, a multi-TeV  $e^+e^-$  collider can access with high precision the triple Higgs coupling, providing experimenters with the opportunity to measure the Higgs potential. The large event statistics will allow physicists to measure rare Higgs decays such as  $H \rightarrow \mu\mu$ . For heavy Higgses, predicted by e.g. supersymmetric models, the range for discovery and measurement will be extended for masses up to and beyond 1 TeV.

- Supersymmetry

In many SUSY scenarios only a subset of the new sparticles will be light enough to be produced directly at a TeV class LC. Some of the heavier sparticles will be discovered at the LHC, but a multi-TeV LC will be needed to complete the spectrum and to precisely measure the heavy sparticles properties (flavor, mass, width, couplings). Furthermore, polarized beams will help disentangle mixing parameters and aid CP studies. Ultimately we *will* need to measure all sparticles as precisely as possible to fully pin down and test the underlying theory.

- New resonances

Many alternative theories and models for new physics predict new heavy resonances with masses larger than 1 TeV. If these new resonances (e.g. new gauge bosons, Kaluza-Klein resonances, or  $W_L W_L$  resonances) have masses in the 1 TeV - 5 TeV range, a multi-TeV collider becomes a particle factory, similar to LEP for the  $Z$ . The new particles can be produced directly and their properties can be accurately determined.

- No new particles

If *no* new particles are observed directly, apart from perhaps one light Higgs particle, then a multi-TeV collider will probe new physics indirectly (extra dimensions,  $Z'$ , contact interactions) at scales in the range of 30-400 TeV via precision measurements.

---

\*timb@slac.stanford.edu; Work supported by Department of Energy contract DE-AC03-76SF00515.

†Albert.de.Roeck@cern.ch

*Presented at the APS/DPF/DPB Summer Study on the Future of Particle Physics (Snowmass 2001),  
30 June - 21 July 2001, Snowmass, Colorado, USA*

- Unexpected phenomena

This is probably the most exciting of all: perhaps Nature has chosen a road as yet not explored (extensively) by our imagination. Recent examples of new ideas are string quantum gravity effects, non-commutative effects, black hole formation, nytons, and split fermions.

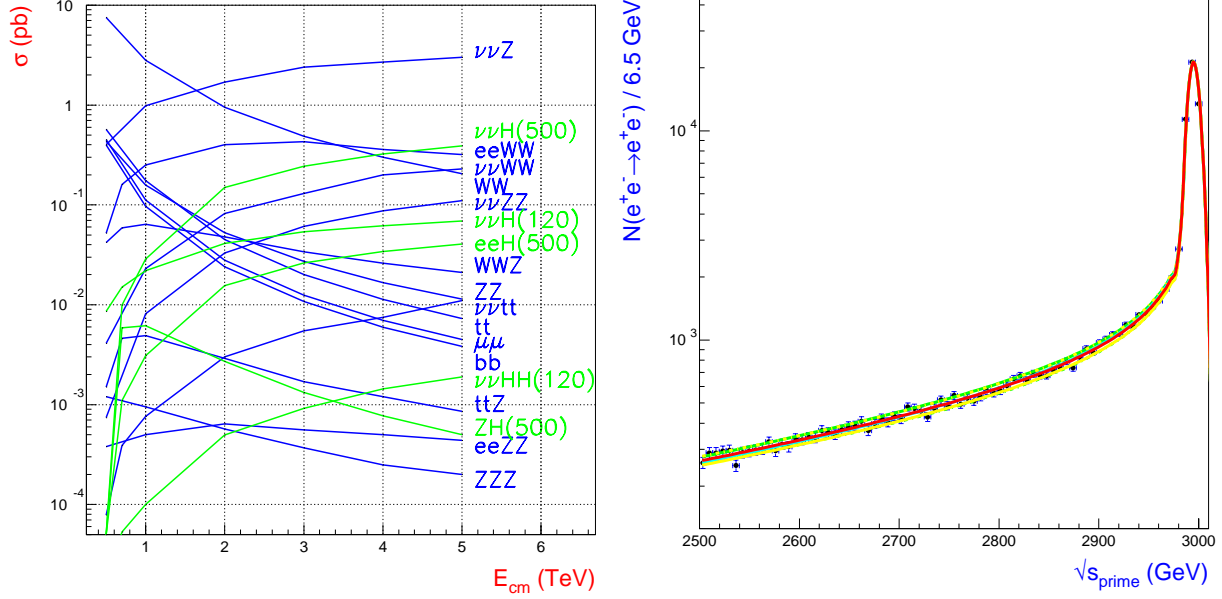


FIG. 1: (Left) Cross sections for several  $s$  and  $t$  channel exchange processes. (Right) Example of a luminosity spectrum at CLIC [5].

TABLE I: Event rates for several processes in the multi-TeV range, for  $1 \text{ ab}^{-1}$  integrated luminosity.

| Event Rates/Year<br>( $1000 \text{ fb}^{-1}$ )          | 3 TeV<br>$10^3$ events | 5 TeV<br>$10^3$ events |
|---|------------------------|------------------------|
| $e^+e^- \rightarrow t\bar{t}$                           | 20                     | 7.3                    |
| $e^+e^- \rightarrow b\bar{b}$                           | 11                     | 3.8                    |
| $e^+e^- \rightarrow ZZ$                                 | 27                     | 11                     |
| $e^+e^- \rightarrow WW$                                 | 490                    | 205                    |
| $e^+e^- \rightarrow hZ/h\nu\nu$ (120 GeV)               | 1.4/530                | 0.5/690                |
| $e^+e^- \rightarrow H^+H^-$ (1 TeV)                     | 1.5                    | 0.95                   |
| $e^+e^- \rightarrow \tilde{\mu}^+\tilde{\mu}^-$ (1 TeV) | 1.3                    | 1.0                    |

An increase of CMS energy needs to be accompanied by an increase of luminosity to compensate for the  $1/s$  dependence of the  $s$ -channel annihilation cross section. However, a feature of the multi-TeV energy range is that the fusion processes ( $t$ -channel exchange), which increase logarithmically with CMS energy, become comparable in strength to the  $s$ -channel annihilation processes, as can be seen in Fig. 1. The event rate of several processes at 3 and 5 TeV CMS energy is given in Table I [5].

The CLIC project at CERN is studying the feasibility of an  $e^+e^-$  linear collider optimized for a CMS energy of 3 TeV with  $\mathcal{L} \cong 10^{35} \text{ cm}^{-2} \text{ s}^{-1}$ , using a novel technique called two-beam acceleration [6]. A so called drive beam of low energy but high current is decelerated, and its energy is transferred to the main low current beam, which gets accelerated with gradients in the range of 100-200 MV/m. The layout of a CLIC accelerator is shown in Fig. 2. With an upgrade program a maximum energy of 5 TeV is foreseen.

In order to reach such high luminosities CLIC will operate in the high beamstrahlungs regime, and the beam parameters and machine requirements are very challenging: nm stability of the components, strong final focus, and 30 GHz accelerating structures. Increasing the luminosity beyond  $10^{35} \text{ cm}^{-2} \text{ s}^{-1}$  will certainly be hard, and probably can only be done by increasing the power and the number of bunches. Likewise, an increase of the energy, e.g. towards 10 TeV, is not excluded but so far only via extending the length of the accelerator.

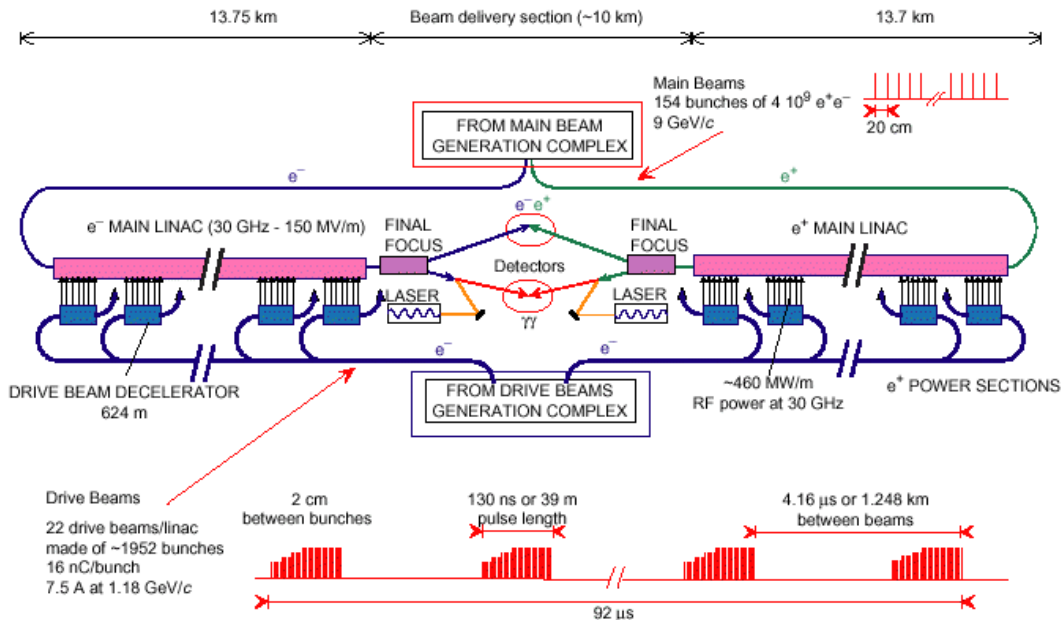


FIG. 2: Overall layout of the CLIC complex for a center-of-mass energy of 3 TeV.

Several test facilities (CTF1, CTF2) [7] have been built over the past 5 years which have succeeded in demonstrating the principle of two beam acceleration. So far, in CTF2 one has reached gradients of 72 MV/m (15 ns pulses, gradient measured with the beam), and 160 MV/m (3 ns pulses, value determined from the power). Furthermore, an X-band structure has been built which achieved 150 MV/m peak accelerating field without beamloading, for 150 ns.

A new test facility, CTF3 [8], is proposed for 2002-2006 and should test the drive beam generation concept. With the knowledge gained at this test facility, if no bad surprises emerge, a conceptual design report for CLIC can be completed in the years afterwards. When it has been decided to develop a full CLIC facility, it is likely to start off with a lower energy version, e.g. with a Higgs factory in  $\gamma\gamma$  mode as discussed in [9], to gain experience with two beam acceleration before making the big leap to the multi-TeV region.

A scheme for an adiabatic upgrade of the JLC/NLC into the multi-TeV region has also been presented [4]. Through the phased installation of a low energy, high current drive beam in the JLC/NLC tunnel, the JLC/NLC could be gradually transformed from an X-band klystron powered accelerator into a two beam accelerator à la CLIC.

A multi-TeV collider will have all the features of a TeV class linear collider, including  $e^-e^-$ ,  $e\gamma$  and  $\gamma\gamma$  collider options. Realizing these options in the multi-TeV region is somewhat more difficult than for a sub-TeV collider, but first studies indicate that the additional complications can probably be overcome [10]. Polarized beam collisions will have an additional loss of 7% of effective polarization during the beam-beam interaction, due to the beamstrahlung and strong fields at 3 TeV [11]. Therefore, polarimeters before and after the collision point will be needed to control this effect. Physics processes might also be used to monitor the effective polarization at the interaction point (IP).

## II. EXPERIMENTAL ENVIRONMENT

The machine parameters [6, 12] needed to achieve these energy and luminosity values lead to important challenges for experiments at CLIC. The beam-beam effects result in considerable backgrounds and a distortion of the luminosity spectrum. An example of a luminosity spectrum is shown in Fig. 1. The effective luminosity available in the peak is given in Table II for different CLIC CMS energies. A list of parameters and backgrounds which will determine the experimental environment at CLIC is given in Table III for 3 TeV and  $\mathcal{L} = 10^{35} \text{ cm}^{-2} \text{ s}^{-1}$ .

The total number of produced  $e^+e^-$  pairs is huge; however the coherent pairs disappear essentially down the beampipe, and the incoherent pairs can be suppressed almost completely if the detector includes a strong magnetic field. These backgrounds force the inner vertex detector to have a minimal inner radius of 3 cm. There are additional backgrounds which need to be taken into account, such as neutrons, muons, and synchrotron

TABLE II: Luminosity within 1% & 5% of  $2 \cdot E_{beam}$  at CLIC

| Energy (TeV)                   | 0.5 | 1    | 3   | 5   |
|--------------------------------|-----|------|-----|-----|
| $\mathcal{L}$ in 1% $\sqrt{s}$ | 71% | 56 % | 30% | 25% |
| $\mathcal{L}$ in 5% $\sqrt{s}$ | 87% | 71 % | 42% | 34% |

TABLE III: Parameters for experimenting at CLIC, for 3 TeV and  $\mathcal{L} = 10^{35} \text{cm}^{-2} \text{s}^{-1}$ .

|  |   |
|--|---|
| Luminosity/bunch   | $10^{-2} \text{ nb}^{-1}$                     |
| Beam energy spread   | 1%(FWHM)                                      |
| bunches per train/ Rep. rate   | 154/100                                       |
| Time between bunches   | 0.67 ns                                       |
| Average energy loss  | 31%   |
| photons/beam particle  | 2.3   |
| Number/energy incoh. pairs   | $4.6 \cdot 10^5 / 3.9 \cdot 10^4 \text{ TeV}$ |
| Number/energy coh. pairs   | $1.4 \cdot 10^9 / 4.4 \cdot 10^8 \text{ TeV}$ |
| Hadronic ( $\gamma\gamma$ ) events, $W_{\gamma\gamma} > 5 \text{ GeV}$ | 4   |

radiation, and these are presently under study [13].

Based on the above machine parameters, the experience at LEP/SLC, and the developments made for TESLA/NLC [14], a first layout for a detector has been worked out. So far the emphasis has been on tracking resolution, jet flavor tagging, energy flow, hermeticity, precise vertexing, and high calorimeter granularity. First ideas for a detector layout at CLIC are given in Table IV, based on a 4T magnetic field. A detector with a 5-6T field, which could be more compact, is considered as well.

However, it is not clear that these lower energy concepts will still be usable at CLIC energies. The multi-TeV high energy frontier opens up new questions such as timing issues ( $< 1 \text{ ns}$  distance between bunches), energy flow (many highly collimated jets), and displaced vertex flavor tagging. The latter is demonstrated in Table V: at  $\sqrt{s} = 3 \text{ TeV}$  the  $B$  mesons produced in  $b\bar{b}$  events decay on average a distance of 9.0 cm from the primary vertex, hence they will decay mostly within or after the vertex detector. For the CLIC physics studies a technique based on multiplicity increase versus distance from the vertex has been developed [15] to search for  $B$ -decays. It has been shown that this technique can tag  $B$  mesons with an efficiency larger than 50% and purity of 85% per jet.

Just as for TeV class linear colliders, the background in the interaction region at CLIC requires the use of a mask. For CLIC the mask covers the region below 120 mrad; electron/photon tagging will be possible down to 40 mrad with detectors in the mask.

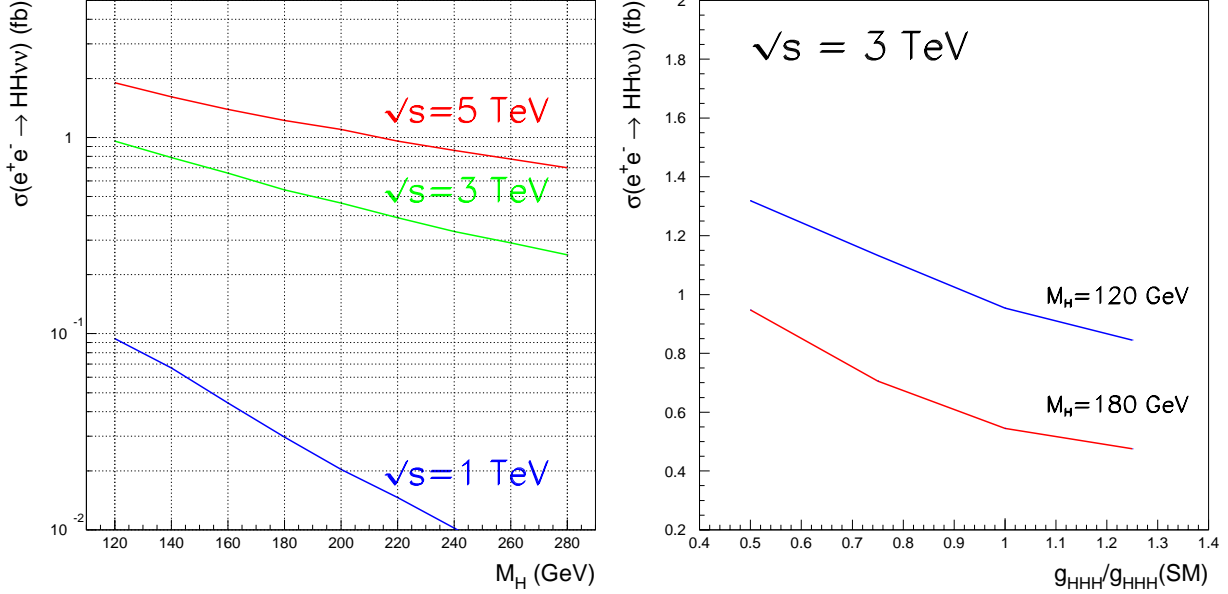
The CLIC physics working group has developed a set of tools to enable physicists to rapidly study physics processes within the multi-TeV experimental environment. The CLIC luminosity spectrum is generated with CALYPSO [13]. The hadronic background from  $\gamma\gamma$  events (4 events/bunch crossing) is generated with HADES [13]. The SIMDET-CLIC fast simulation package is used (based on the package for the TESLA Detector [16]). The adapted VECSUB package for jet reconstruction is used (DURHAM, JADE algorithms) [17] for analysis. Most of the studies discussed in this paper are based on these tools.

TABLE IV: Design concept (detector layers) for a detector at CLIC

|            |                               |
|------------|-------------------------------|
| 3–15 cm    | Silicon VDET                  |
| 15–80 cm   | Silicon central/forward disks |
| 80–230 cm  | TPC or Silicon tracker        |
| 240–280 cm | ECAL ( $30 X_0$ )             |
| 280–400 cm | HCAL ( $6\lambda$ )           |
| 400–450 cm | Coil (4T)                     |
| 450–800 cm | Fe/muon                       |

TABLE V: B-decay length in space at different CMS energies, and for several processes.

| $\sqrt{s}$ (TeV) | 0.09 | 0.2  | 0.35 | 0.5  | 3.0                   |
|------------------|------|------|------|------|-----------------------|
|                  | $Z$  | $HZ$ | $HZ$ | $HZ$ | $H^+H^-$   $b\bar{b}$ |
| $d_{space}$ (cm) | 0.3  | 0.3  | 0.7  | 0.85 | 2.5   9.0             |

FIG. 3: (Left)  $\sigma_{HH\nu\nu}$  as function of  $M_H$  for a LC with  $\sqrt{s} = 0.5, 1$  and  $3$  TeV. (Right) Change of the cross section for  $e^+e^- \rightarrow HH\nu\nu$  as function of the change of the coupling  $g_{HHH}$  [18].

### III. HIGGS PHYSICS

Within the SM the circumstantial evidence for a light Higgs is accumulating, offering the TeV class LCs an exciting physics program to study in detail the Higgs properties. However – perhaps at first sight surprisingly – a multi-TeV can add substantial and important information about a light Higgs.

A final proof of the Higgs mechanism, which may still be unsettled after the TeV class LC data has been collected, is the accurate reconstruction of the potential of the Higgs field. The Higgs potential  $V$  can be studied through triple ( $g_{HHH}$ ) and quartic Higgs couplings:

$$V = \lambda v^2 H^2 + \lambda v H^3 + \frac{1}{4} \lambda H^4, \quad M_H = \sqrt{2} \lambda v, \quad g_{HHH} = 3 \lambda v, \quad (1)$$

where  $H$  is the Higgs field,  $M_H$  is the Higgs mass and  $v = 246$  GeV is the Higgs vacuum expectation value parameter. An accurate measurement of this relation would probe the extended nature of the Higgs sector, and is therefore of fundamental importance.

The triple Higgs coupling can be studied in double Higgsstrahlung,  $e^+e^- \rightarrow HHZ$ , and in the fusion process  $e^+e^- \rightarrow HH\nu\nu$ . Only the second process is relevant for multi-TeV colliders. The cross section as a function of the Higgs mass is shown in Fig. 3 for several LC CMS energy values: the cross section is very strongly CMS energy dependent. Together with the larger luminosity expected for a multi-TeV collider, this will lead to event samples which are up to a factor of 100 larger than at a TeV class collider.

A study including detector acceptance, smearing and background was performed for  $4b$  ( $M_H = 120$  GeV) and  $4W$  ( $M_H = 180$  GeV) final states [18]. The statistical precision on  $g_{HHH}$  with  $5 \text{ ab}^{-1}$  and a CMS energy of 3 TeV from a measurement of the  $HH\nu\nu$  cross section for  $M_H = 120(180)$  GeV is  $\delta g_{HHH}/g_{HHH} = 0.094(0.140)$ . By making use of the scalar nature of the Higgs decay these limits can be improved to  $\delta g_{HHH}/g_{HHH} = 0.070(0.080)$  for  $M_H = 120(180)$  GeV. Clearly this channel will be statistics limited. The use of polarized beams could yield up to a factor of about 4 more in statistics. No other machine presently considered could reach this kind of precision in the triple Higgs coupling. Fig. 3 shows the dependence of the  $HH\nu\nu$  cross section on the triple Higgs coupling, normalized to its SM value, for  $\sqrt{s} = 3$  TeV and two values of  $M_H$ .

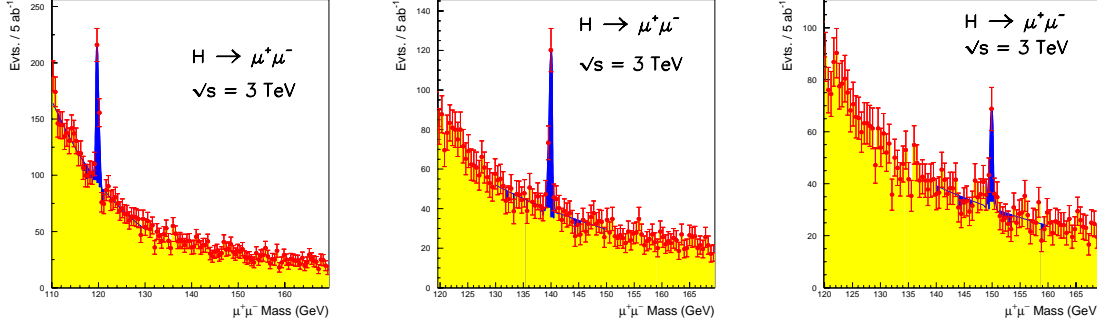


FIG. 4: The  $\mu\mu$  invariant mass spectrum for background and signal  $H \rightarrow \mu\mu$  for different values of  $M_H$  [19].

The benefit of an increasing event rate with increasing CMS energy does not continue indefinitely, due to the competition of background processes which have the same final state but no triple Higgs vertex, and due to the forward nature of the produced Higgs pairs, which become increasingly more difficult to detect. Studies indicate that the optimal CMS energy for a maximum sensitivity to the triple Higgs coupling is between 2.5 and 4 TeV, depending on the Higgs mass.

The quartic Higgs coupling remains unfortunately elusive. The cross section for  $ee \rightarrow HHH\nu\nu$  is about three orders of magnitude smaller than for  $ee \rightarrow HH\nu\nu$ . Hence, at a 3 TeV collider one expects only 0.4 events produced per year. In the most favorable condition of a 10 TeV collider and  $10^{35}\text{cm}^{-2}\text{s}^{-1}$ , one would produce only 5 signal events per year, so that even the prospect for exploratory studies looks rather dim.

Apart from the Higgs potential, a multi-TeV collider also provides physicists with the opportunity to measure rare decay modes of the Higgs. For example, the decay  $H \rightarrow \mu\mu$  has a branching ratio of about  $10^{-4}$  in the SM for a light Higgs. Its measurement is one of the driving motivations for a muon collider. For  $5\text{ab}^{-1}$  at 3 TeV,  $2.7 \times 10^6$  Higgs bosons with  $M_H = 120$  GeV will be produced, of which 650 will decay into muons. Including detector smearing and acceptance leads to a di-muon invariant mass spectrum as shown in Fig. 4 [19]. The measurement of this cross section can be combined with an independent measurement of the Higgs production cross section, e.g. via the  $b$  or  $W$  decay modes, to extract  $g_{H\mu\mu}$ . The statistical accuracy of the measurement of the coupling  $g_{H\mu\mu}$  can be  $\delta g_{H\mu\mu}/g_{H\mu\mu} = 0.040, 0.062, \text{ and } 0.106$ , for Higgs masses of 120, 140, and 150 GeV, respectively. Hence the anticipated accuracy of this measurement is comparable to that predicted at a muon collider [20], and better than present expectations for a VLHC at 200 TeV [21]. Note that for this channel the production is rather forward, so that a further increase in CMS energy does not translate completely to a corresponding increase in precision.

With the measurement of this branching ratio one can verify the Higgs mechanism in the lepton sector – specifically the relation  $g_{H\mu\mu}/g_{H\tau\tau} = M_\mu/M_\tau$  – with a precision of 5-8% for a Higgs mass in the range of 120-140 GeV. Any striking anomalous behaviour in the muon channel would be easily detectable.

In minimal SUSY scenarios a total of 5 Higgs particles is expected. One light neutral higgs is expected, typically with a mass below 130 GeV, while the masses of the others Higgses are usually degenerate and depend strongly on the SUSY parameters of the model. Scenarios have emerged where the heavy Higgses are larger than 500 GeV, and therefore cannot be pair produced at a 1 TeV LC. Some gain in reach can be obtained, up to about  $M_H = 700$  GeV, using the LC in the  $\gamma\gamma$  mode.

For CLIC the process  $e^+e^- \rightarrow H^+H^-$  with  $M_H = 880$  GeV has been studied. A scenario including heavy Higgs masses around this value is given by point (J) in the newly proposed SUSY benchmarks [22], discussed in the next section. The decay channel  $H^\pm \rightarrow tb \rightarrow Wbb \rightarrow qqbb$  has been studied in which eight jets are expected in the final state [23]. Events are selected where both Higgses are reconstructed. The tagging of  $b$ -quarks will be extremely important for such an analysis. The cross section is shown in Fig. 5. Using the kinematic constraints of the  $W$  and  $t$  masses to disentangle the jet pairing, events with two heavy Higgses can be selected. An overall kinematic fit, taking into account the effects of the overlaid  $\gamma\gamma$  events, can improve the Higgs mass resolution by a factor two, leading to a resolution of 33 GeV which can be compared to the natural width of the  $H^\pm$  of 21 GeV. The result is shown in Fig. 5, for a study including 15 bunch crossings with  $\gamma\gamma$  events overlaid. A total of 47 reconstructed events of the type  $e^+e^- \rightarrow H^+H^- \rightarrow (t\bar{b})(\bar{t}b)$  is expected in the mass region of  $2.5\sigma$  around the peak. From these and follow up studies we find that a  $5\sigma$  discovery can be made at a 3 TeV collider with  $3\text{ab}^{-1}$  for a Higgs mass up to about 1.1 TeV. Once the heavy Higgs has been discovered one can increase the efficiency (now a only few %) and hence the number of heavy Higgs particles by using a mass window and requiring only (at least) one Higgs per event.

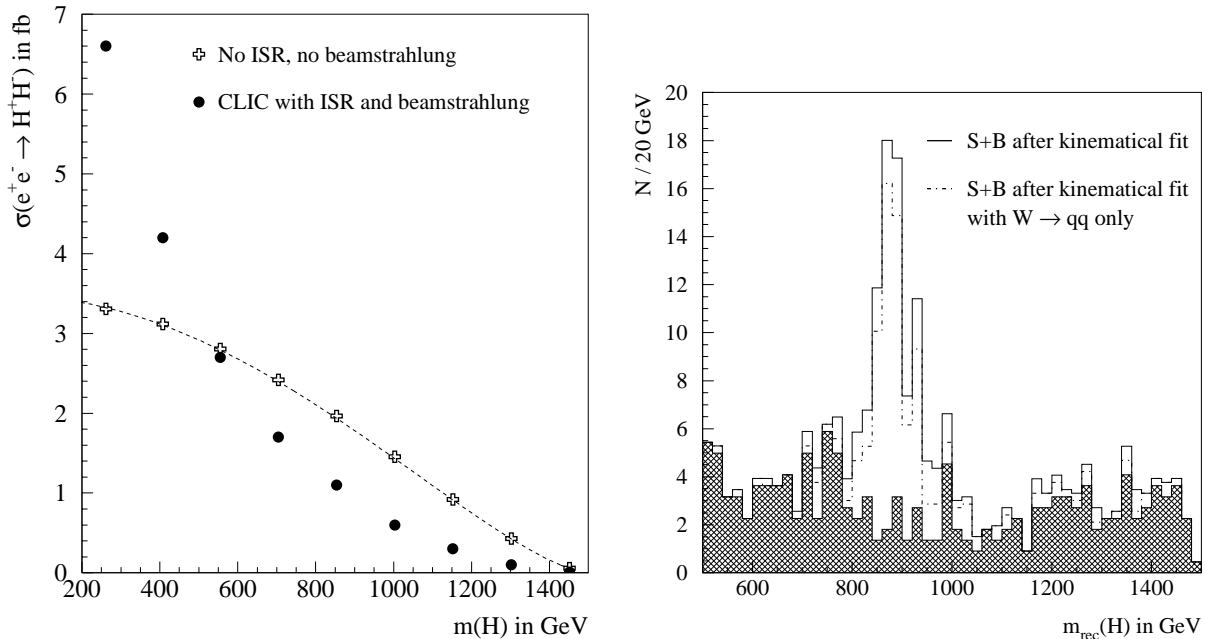


FIG. 5: (Left) Cross section for  $e^+e^- \rightarrow H^+H^-$  at  $\sqrt{s} = 3$  TeV. Open crosses and dashed lines show the cross section at tree level, while full circles show the effective cross section after including ISR and beamstrahlung. (Right) Reconstructed  $H^\pm \rightarrow tb$  invariant mass after the kinematical fit for an integrated luminosity of  $3 \text{ ab}^{-1}$ . The  $t\bar{t}b\bar{b}$  background is shown by the hatched distribution[23].

In short a multi-TeV collider will add new information on the measurement of the Higgs potential, rare Higgs decays, and heavy Higgs states.

#### IV. SUPERSYMMETRY

A strong candidate for new physics, which would explain the hierarchy problem, is supersymmetry. This new symmetry predicts a partner for each known particle, a “sparticle”. Since no sparticles have been observed so far supersymmetry is broken at the electroweak scale, and there are many models proposed for the supersymmetry breaking mechanism. These supersymmetry breaking models reduce the more than 100 new parameters that enter the theory to only a handful. All of these models predict a different phenomenology, including different mass spectra for the supersymmetric partners. Sparticles can be readily discovered at an  $e^+e^-$  machine so long as direct production is kinematically allowed.

Studies for future facilities rely on benchmark points. The benchmark points used in previous studies have by now been mostly ruled out by the final measurements at LEP and the Tevatron. Recently a new set of benchmark points has been suggested in [22]. This study is based on the constrained MSSM model and takes into account the experimental search limits on sparticles, Higgs bosons,  $\tan\beta$ ,  $b \rightarrow s\gamma$  results, the compatibility with Dark Matter ( $0.1 < \Omega h^2 < 0.3$ ), and, for some points, the compatibility with  $g-2$ . The model parameters  $m_{1/2}, m_0, \tan\beta$ , sign of  $\mu$  have been varied, while in order to not inflate the parameter space too much only points with  $A = 0$  have been chosen. An overview of the selected points in the  $m_0, m_{1/2}$  plane is given in Fig. 6. The light coloured regions in which the points are shown, are the allowed regions; these include regions towards large  $m_{1/2}$  with fast coannihilation regions, a rapid annihilation funnel, and a focus point region close to the border of the region where electroweak symmetry breaking is no longer possible. Note that the points are chosen to span a large part of the phase space, including the more extreme corners, and cover  $\tan\beta$  values from 5 to 50. Some of the points are  $3\sigma$  away from the value of  $g-2$  that was reported in early 2001, and have large fine tuning values. Hence, these points do *not* represent a sampling of the region according to the ‘likeliness’ or compatibility with constraints, but rather represent a collection of different scenarios, and are thus not meant for a statistical study.

All of the scenarios proposed in [22] are found to have sparticles with masses larger than 500 GeV. Thus, a LC with an energy above 1 TeV would be needed to study all sparticles in  $e^+e^-$  collisions. An example of the

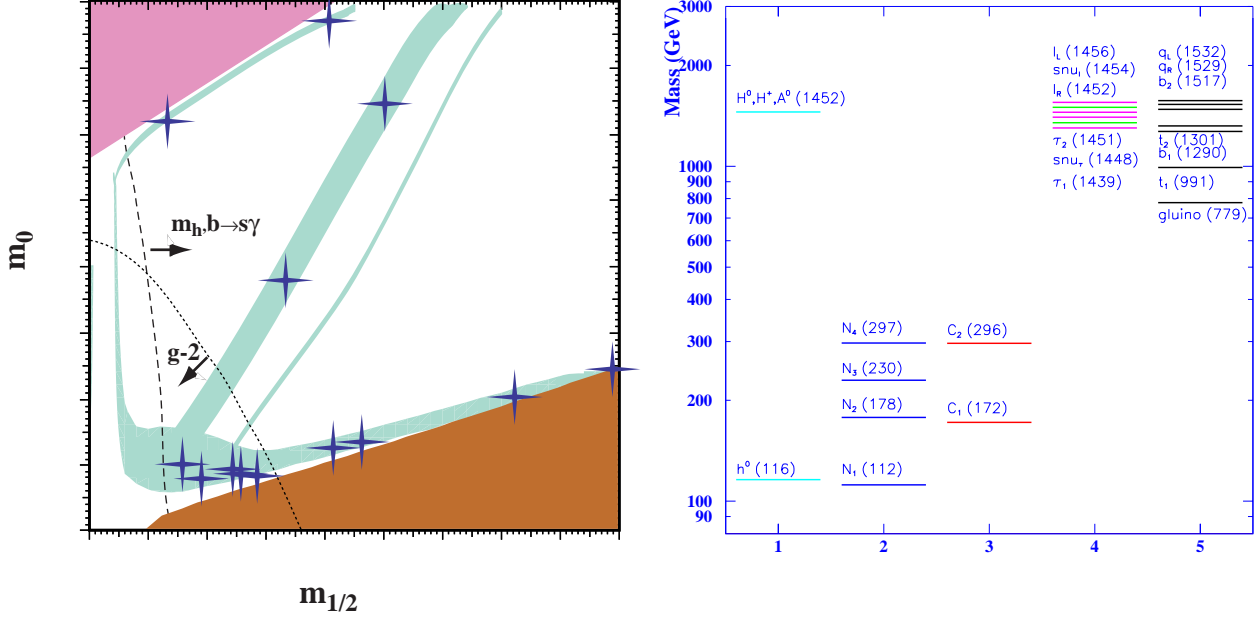


FIG. 6: (Left) Qualitative overview of the locations the proposed CMSSM benchmark points in a generic  $(m_{1/2}, m_0)$  plane. (Right) Example of a mass spectrum for point E of [22].

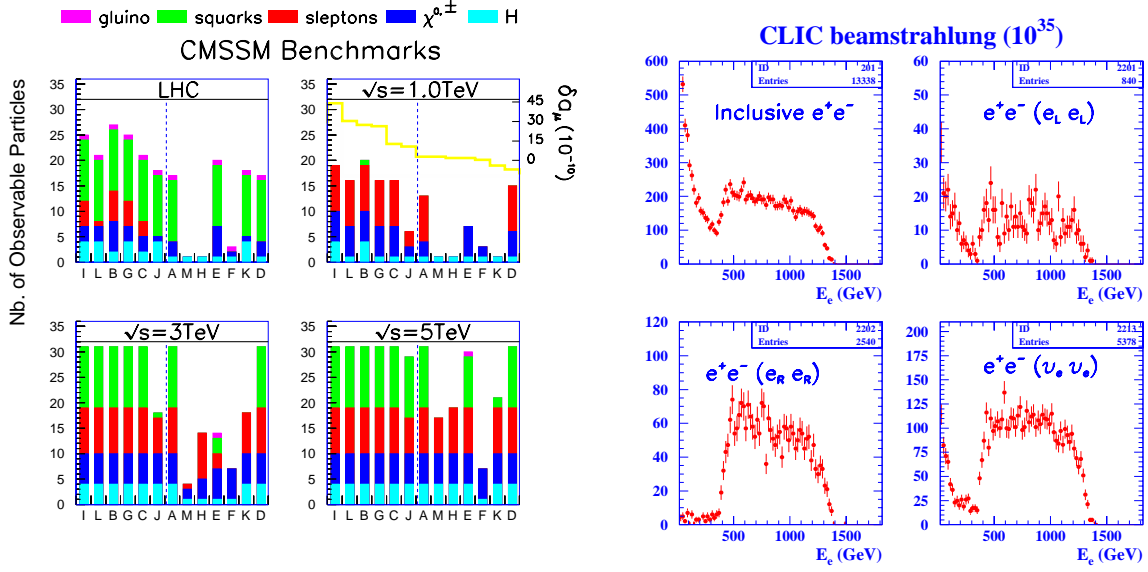


FIG. 7: (Left) Comparison of the capabilities of various colliders to observe different species of supersymmetric particles, in a range of supersymmetric models whose parameters are chosen to be compatible with experimental constraints from LEP and elsewhere. The models are ordered by their degree of compatibility with the recent BNL measurement of the muon anomalous magnetic moment, as indicated by the line in the top right panel. We see that linear colliders complement the LHC, via their abilities to observe weakly-interacting sparticles, in particular. In most of the restricted set of simplified models studied, CLIC (almost) completes the supersymmetric spectroscopy initiated by the LHC. (Right) Measured electron and positron spectrum for inclusive di-electron events for point E, for  $\sqrt{s} = 3.5\text{ TeV}$  and  $650\text{ fb}^{-1}$  using SPYHTIA, CALYPSO and SIMDET. Panels 2, 3 and 4 show the di-electron events from  $\tilde{e}_L \tilde{e}_L$ ,  $\tilde{e}_R \tilde{e}_R$  and  $\tilde{\nu}_e \tilde{\nu}_e$  assuming ideal process separation [22, 26].

mass spectrum is shown in Fig. 6 for point (E) of [22], corresponding to  $m_{1/2} = 300$  GeV,  $m_0 = 1450$  GeV,  $\tan\beta = 10$ , sign of  $\mu > 0$  and  $A = 0$ . For this point the heavy Higgses, sleptons and squarks have masses larger than 700 GeV.

We do not yet know which, if any, SUSY scenario is realized in Nature and where we should search for the SUSY particles. The LHC will certainly tell us if SUSY particles exist at the TeV scale, but the chances are large that at least some of the sparticles will be out of reach at a 1 TeV collider. Sooner or later the need will arise to measure as precisely as possible *all* members of the sparticle spectrum, in order to disentangle the underlying theory and (SUSY breaking) dynamics as completely as possible. It has been shown for TeV class LC SUSY sparticle measurements, that knowing the masses to a level better than 1% rather than about 10% (typical for the LHC) is an enormous help for bottom-up approaches to reconstruct the SUSY breaking mechanism [24]. Another important aspect of  $e^+e^-$  linear colliders is initial state beam polarization, which can be used to single out newly produced states of definite helicity, and further disentangle SUSY parameters [25].

Since supersymmetry will have been discovered (or possibly refuted) already before the turn on of a multi-TeV collider, its main task could be to complete the sparticle spectrum with precise measurements. The number of particles which can be detected at a LC and LHC for the chosen SUSY benchmark points is shown in Fig. 7. For a sparticle to be observed at a LC, its cross section has to be larger than  $0.1 \text{ fb}^{-1}$ . The points are ordered according to decreasing value of their compatibility with  $g - 2$ . For the ‘ $g - 2$  friendly’ points the LHC can detect the squarks, and a 1 TeV collider can often detect sleptons and gauginos, and sometimes also the heavy Higgs particles. The notion of ‘ $g - 2$  friendly’ is, however, somewhat changing with time.

A multi-TeV collider can almost always produce all sparticles, except the gluino, for  $g - 2$  friendly points, and also quite a few sparticles from points in the  $g - 2$  ‘unfriendly’ region. It is clear that with our present lack of knowledge of the mass pattern of the sparticles, the option to upgrade a multi-TeV collider like CLIC to 5 TeV must be kept. Moreover, Fig. 7 shows that even a 5 TeV collider will not cover the full phase space of presently allowed scenarios. In order to cover all points proposed in [22] –which does not necessarily give the upper limit of the possible particle mass range either– a  $e^+e^-$  collider of 8 TeV would be necessary, and the luminosity would need to be increased by a factor 2-5 to produce measurable samples of all sparticles.

Next one needs to study the question whether a machine like CLIC, with its important backgrounds and luminosity spectrum smearing can make precision measurements of sparticle properties. A case study is shown in Fig. 7 for sneutrino pair production and the sneutrino mass determination for point (E) above. The signal is  $\tilde{\nu}_e \tilde{\nu}_e \rightarrow e^+ \tilde{\chi}_1^- e^- \tilde{\chi}_1^+$  [26]. The study relies on the typical ‘box’ shape of the inclusive lepton spectrum, a technique developed for a TeV class LC: the end points of the rectangular shape in Fig. 7 determine the slepton and gaugino mass. The study includes background processes and machine background effects. The figure shows that the signal is preserved in the CLIC environment. A recent study [27] shows that mass measurements for smuons are possible with a precision of  $O(1\%)$ .

In general the gluino is difficult to measure at an  $e^+e^-$  LC, except when it is lighter than the squarks. A possible way to measure gluinos is via the  $\gamma\gamma$  collider option. In [28] it was shown that gluinos are produced with cross sections which are a few orders of magnitude larger than in  $e^+e^-$  collisions. Gluinos could be detected at a 3 TeV collider in the  $\gamma\gamma$  mode for masses up to about 1 TeV, where they are produced with cross sections in the range of  $1\text{--}0.1 \text{ fb}^{-1}$ , if the gluinos are heavier than the squarks. Hence the initial studies indicate that if SUSY is stabilizing the SM, and sparticles have masses in the anticipated range, then a multi-TeV  $e^+e^-$  collider would be the ideal tool to complete the sparticle spectrum.

## V. $e^+e^- \rightarrow f\bar{f}$ AND PRECISION MEASUREMENTS

Extending the sensitivity of new physics beyond the reach of the LHC is a prime aim for a future collider. LEP has demonstrated how an  $e^+e^-$  collider can provide precision measurements, and be a powerful tool for searching for new physics. Reactions at  $e^+e^-$  colliders are simple, clean, and precisely calculable. These features enable an  $e^+e^-$  collider to match, and in many instances surpass, the energy scale reach of contemporaneous higher energy hadron colliders.

There is a wide range of new physics scenarios predicting the existence of new vector particles with masses in the TeV range. These basically aim at explaining the origin of electroweak symmetry breaking if there is no light elementary Higgs boson, stabilizing the SM if SUSY is not realised in Nature, or embedding the SM in a theory of grand unification.

One of the simplest extensions of the SM involves the introduction of an additional  $U(1)$  gauge symmetry, whose breaking scale is close to the Fermi scale, leading to new gauge bosons. Several models for the production of new  $Z'$  bosons have been studied for a multi-TeV collider [30]. First we study the case of direct production of such new bosons, which will produce a resonance signal in the two-fermion production processes, just like the  $Z$  at LEP. The LHC could also produce such bosons with a detectable rate in the range up to a few TeV,

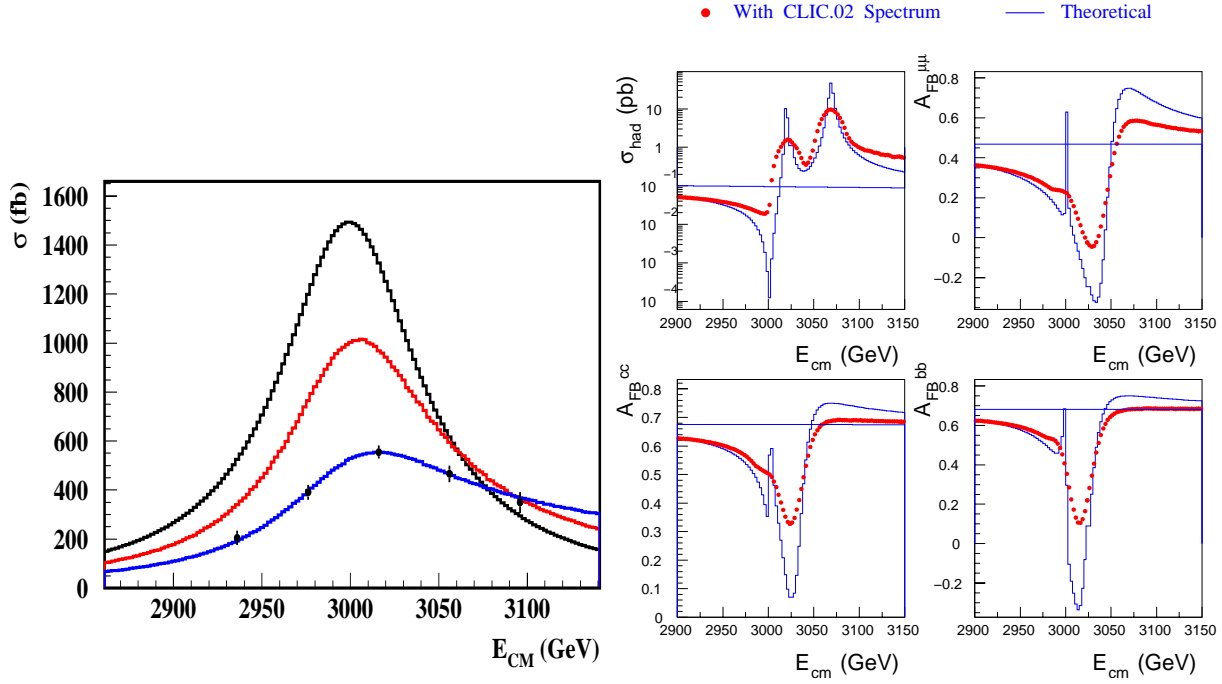


FIG. 8: (Left) Production of  $Z' \rightarrow l^+l^-$  shown at the Born level (top), including ISR (middle) and further including smearing due to the luminosity spectrum. (Right) Hadronic cross section and Forward-Backward asymmetries at energies around 3 TeV. Continuous lines are predictions by the D-BESS model with  $M = 3$  TeV and  $g/g'' = 0.015$ , and dots the observable D-BESS signal after including smearing of the luminosity spectrum [30].

TABLE VI: Sensitivity to  $L_3$  and  $R_3$  production at the LHC ( $\mathcal{L} = 500 \text{ fb}^{-1}$ ) and CLIC ( $\mathcal{L} = 1 \text{ ab}^{-1}$ ).

| $g/g''$ | $M$<br>(GeV) | $\Gamma_{L_3} / \Gamma_{R_3}$<br>(GeV) | $S/\sqrt{S+B}$<br>LHC ( $e + \mu$ ) | $S/\sqrt{S+B}$<br>CLIC (had.) | $\Delta M$<br>CLIC |
|---------|--------------|--|-------------------------------------|-------------------------------|--------------------|
| 0.1     | 3000         | 2.0 / 0.3                              | 3.4                                 | 62                            | $23.20 \pm .06$    |
| 0.2     | 3000         | 8.2 / 1.2                              | 6.6                                 | 152                           | $83.50 \pm .02$    |

but it will not have the statistical power to measure in detail their properties.

For the multi-TeV collider study we assume a new gauge boson with  $M_{Z'}$  of 3.0 TeV and a width  $\Gamma(Z')/M_{Z'} \simeq \Gamma(Z^0)/M_{Z^0}$ . A ‘LEP-like’ scan of the cross section in five points, as shown in Fig. 8, for a total of  $1 \text{ ab}^{-1}$  at CLIC gives the following fit accuracy:  $\delta M_{Z'}/M_{Z'} \sim 10^{-4}$  and  $\delta \Gamma_{Z'}/\Gamma_{Z'} \sim 3 \cdot 10^{-3}$ . The precision is somewhat worse than the one obtained for the  $Z$  at LEP, but would still be a textbook measurement.

Some of these models, such as the degenerate BESS Model, predict several almost degenerate resonances in the multi-TeV region. Disentangling these resonances and measuring their properties will be particularly challenging. For example, in the degenerate BESS model one expects two almost degenerate triplets:  $L_3, L_3^\pm$  and  $R_3, R_3^\pm$ . The sensitivity to  $L_3$  and  $R_3$  with  $M = 3$  TeV for  $\mathcal{L} = 500 \text{ fb}^{-1}$  at LHC and  $\mathcal{L} = 1 \text{ ab}^{-1}$  at CLIC are given in Table VI. A possible energy scan of narrow resonances is shown in Fig. 8 for the case of  $g/g'' = 0.15$ , with  $g''$  the coupling corresponding to the additional symmetry. The studies show that CLIC can distinguish resonances with a  $\Delta M$  down to 13 GeV, corresponding to  $g/g'' > 0.08$  in this model.

Also, the direct production of new gauge bosons in the Left-Right symmetric model has been studied [29]; in particular the production of a  $Z'$  with a mass of 3 TeV which decays into heavy Majorana neutrinos. This leads to multi-jet plus lepton final states. The large number of  $Z' \rightarrow N_e N_e$  events can be used to determine the masses of these new particles with an accuracy of 0.01% for the  $Z'$  and 0.19% for the heavy neutrino.

Apart from the direct observation of new resonances, signals of this kind of new physics at even higher energy scales can be discovered in precision measurements of two fermion production processes. The sensitivity to new physics of LEP observables such as  $\sigma_{f\bar{f}}$ ,  $A_{\text{FB}}^{f\bar{f}}$  and  $A_{\text{LR}}^{f\bar{f}}$  has been studied with the CLIC tools. The statistical accuracy for the determination of  $\sigma_{f\bar{f}}$ ,  $A_{\text{FB}}^{f\bar{f}}$  and  $A_{\text{LR}}^{f\bar{f}}$  has been determined, for  $\mu^+\mu^-$  and  $b\bar{b}$ , taking

TABLE VII: Relative statistical accuracies on electroweak observables, obtained for  $1 \text{ ab}^{-1}$  of CLIC data at  $\sqrt{s} = 3 \text{ TeV}$ , including the effect of  $\gamma\gamma \rightarrow \text{hadrons}$  background.

| Observable            | Relative Stat. Accuracy<br>$\delta\mathcal{O}/\mathcal{O}$ for $1 \text{ ab}^{-1}$ |
|-----------------------|--|
| $\sigma_{\mu^+\mu^-}$ | $\pm 0.010$  |
| $\sigma_{b\bar{b}}$   | $\pm 0.012$  |
| $A_{FB}^{\mu\mu}$     | $\pm 0.018$  |
| $A_{FB}^{bb}$         | $\pm 0.055$  |

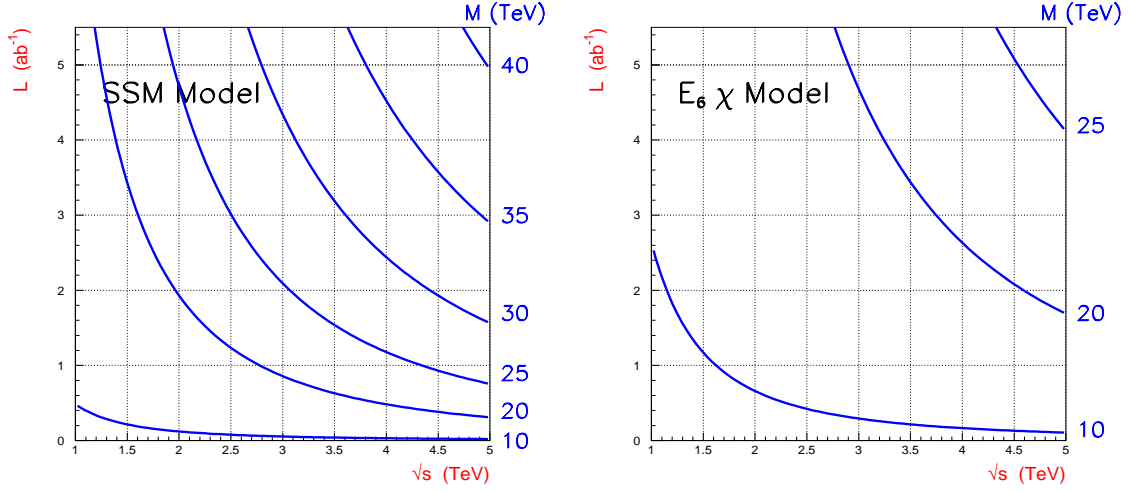


FIG. 9: The 95% C.L. sensitivity contours in the  $\mathcal{L}$  vs.  $\sqrt{s}$  plane for different values of  $M_{Z'}$  in the SSM model (left) and in the  $E_6 \chi$  model (right) [30].

the CLIC parameters at  $\sqrt{s} = 3 \text{ TeV}$ . The relative statistical accuracies for these observables,  $\delta\mathcal{O}/\mathcal{O}$ , are given in Table VII. Note that these estimations take full account of the background at CLIC.

The sensitivity to search for indirect signals of  $Z'$  bosons increases with luminosity and available CMS energy:

$$M_{Z'} \propto \sqrt{s \frac{\sigma}{\delta\sigma}} \propto \sqrt{s \sqrt{\frac{\mathcal{L}}{s}}} = (s \times \mathcal{L})^{1/4}. \quad (2)$$

Hence a 5 TeV collider with  $\mathcal{L} \cong 10^{35} \text{ cm}^{-2} \text{ s}^{-1}$  can achieve a factor 3 to 4 more in discovery reach compared to a TeV class collider. These scaling laws have been verified by detailed studies using the accuracies of the two-fermion related measurements as given in Table VII. The results based on the detailed studies, for two different models which produce a  $Z'$ , are shown in Fig. 9. For the SSM model, a region up to  $M_{Z'} = 40 \text{ TeV}$  can be covered for  $5 \text{ ab}^{-1}$  [30].

The studies above have addressed specific models of new physics beyond the SM. Fermion compositeness or exchange of very heavy new particles can be described more generally by four-fermion contact interactions [31]. These parameterize the interactions beyond the SM by means of an effective scale,  $\Lambda$ ,

$$\mathcal{L}_{CI} = \sum_{i,j=L,R} \eta_{ij} \frac{g^2}{\Lambda_{ij}^2} (\bar{e}_i \gamma^\mu e_i) (\bar{f}_j \gamma^\mu f_j). \quad (3)$$

By convention one usually takes  $g^2/4\pi = 1$ , and scenarios with different chirality are distinguished from one another by specifying values of  $\pm 1$  or 0 for the coefficients  $\eta_{ij}$ . The contact scale  $\Lambda$  can then be interpreted as the mass of the new particles exchanged by the strongly interacting fermion constituents.

The sensitivity of electroweak observables to the contact interaction scale  $\Lambda$  was estimated using the statistical accuracies in Table VII for the  $\mu\mu$  and  $b\bar{b}$  final states. Beam polarization represents an important tool in these studies. First, it improves the sensitivity to new interactions through the introduction of the left-right asymmetries  $A_{LR}$  and the polarized forward-backward asymmetries  $A_{FB}^{pol}$  in the electroweak fits. If both beams

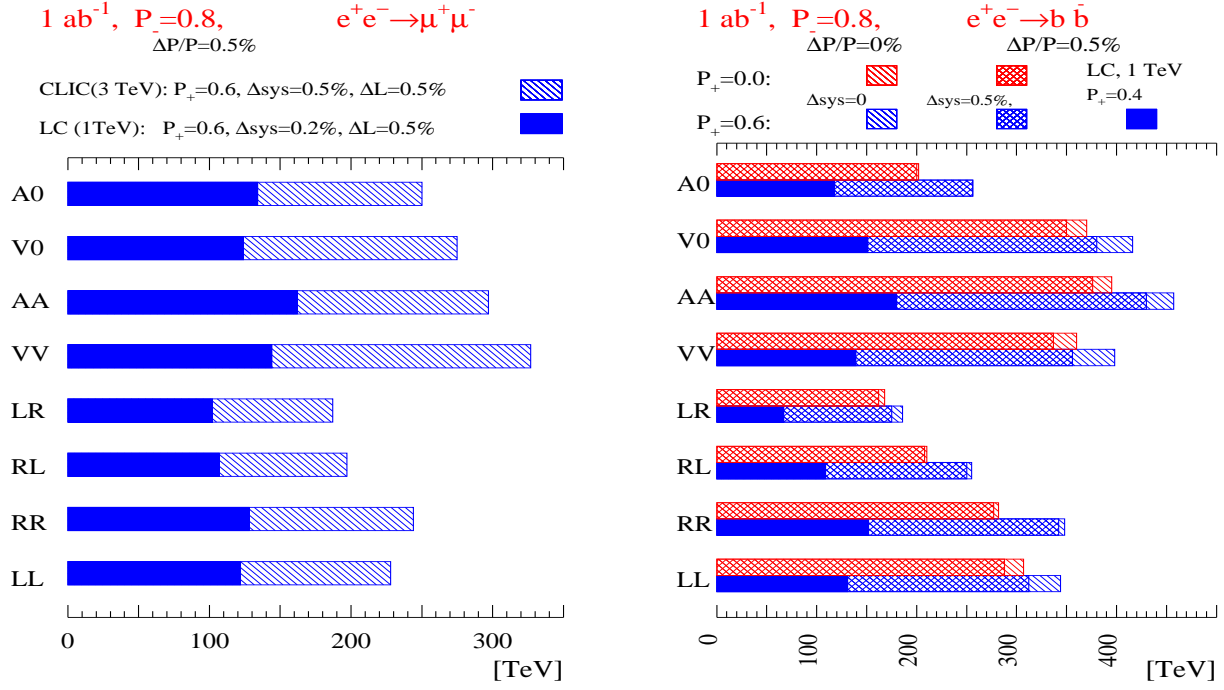


FIG. 10: Limits on the scale  $\Lambda$  of contact interactions in  $ee \rightarrow \mu\mu, b\bar{b}$  for CLIC operating at 3 TeV (dashed histogram) compared to a 1 TeV LC (filled histogram) for different models and the  $\mu^+\mu^-$  (left) and  $b\bar{b}$  (right) channels. The electron polarizations  $\mathcal{P}_-$  is taken to be 0.8 and the positron  $\mathcal{P}_+$  to be 0.6. For comparison the upper bars in the right plot show the sensitivity achieved without positron polarization [30].

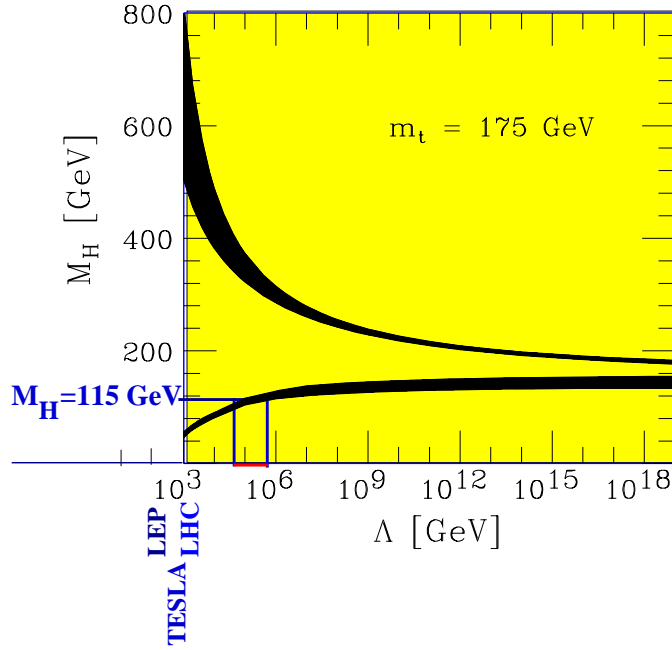


FIG. 11: The range allowed for the mass of the Higgs boson if the SM is to remain valid up to a given scale  $\Lambda$ . In the upper part of the plane, the effective potential blows up, whereas in the lower part the present electroweak vacuum is unstable [32].

can be polarized to  $\mathcal{P}_-$  and  $\mathcal{P}_+$  respectively, the relevant parameter is the effective polarization defined as  $\mathcal{P} = (-\mathcal{P}_- + \mathcal{P}_+)/(\mathcal{P}_- + \mathcal{P}_+)$ . In addition to the improved sensitivity, the uncertainty on the effective polarization, can be made smaller than the error on the individual beam polarization measurements. Secondly, in the case that a significant deviation from the SM prediction is observed,  $e^-$  and  $e^+$  polarization would be useful in determining the helicity structure of the new interactions.

Results are given in Fig. 10 in terms of lower limits on  $\Lambda$  which can be excluded at 95% C.L. High luminosity  $e^+e^-$  collisions at 3 TeV can probe  $\Lambda$  scales in the range 200-400 TeV for  $1 \text{ ab}^{-1}$ . For comparison, the corresponding results expected for a LC operating at 1 TeV are also shown [30]. Using the scaling law, the expected gain in reach on  $\Lambda$  for  $5 \text{ ab}^{-1}$  and a 5 TeV (10 TeV)  $e^+e^-$  collider would be 400-800 GeV (500-1000) TeV. This is a very exciting prospect, *if* the ‘doomsday’ scenario is encountered, where some years from now only a light Higgs has been discovered, and no sign of other new physics has been revealed by the LHC or a TeV class LC. Indeed, if the Higgs particle is light, i.e. below 150 GeV or so, then the Standard Model cannot be stable up to the GUT or Planck scale, and a new mechanism is needed to stabilize it as shown in Fig. 11 [32]: only a narrow corridor up to the Planck scale is allowed for Higgs masses around 180 GeV. For example, for a Higgs with a mass in the region of 115-120 GeV, the SM will hit a region of electroweak unstable vacuum in the range of 100-1000 TeV. Hence, if the theory assessment of Fig. 11 remains valid, and the bounds do not change significantly (which could happen due to a change in the top-mass from e.g. new measurements at the Tevatron) *and* the Higgs is as light as 120 GeV, then the signature of new physics cannot escape precision measurements at a multi-TeV collider.

Another example of precision measurements is the determination of triple gauge boson couplings, studied e.g. via  $e^+e^- \rightarrow W^+W^-$ . Deviations from the SM expectations in these couplings are a sign of new physics. An initial study, using TeV class LC results for background and detector effects, suggests that the sensitivity of the anomalous  $\Delta\lambda_\gamma$  and  $\Delta\kappa_\gamma$  couplings (which are zero in the SM) for CLIC at 3 (5) TeV amounts to roughly  $1.3 \cdot 10^{-4}$  ( $0.8 \cdot 10^{-4}$ ) and  $0.9 \cdot 10^{-4}$  ( $0.5 \cdot 10^{-4}$ ) respectively, for  $1 \text{ ab}^{-1}$  of data [33]. Hence a multi-TeV collider can probe these couplings a factor 2-4 times more precisely than a TeV class LC.

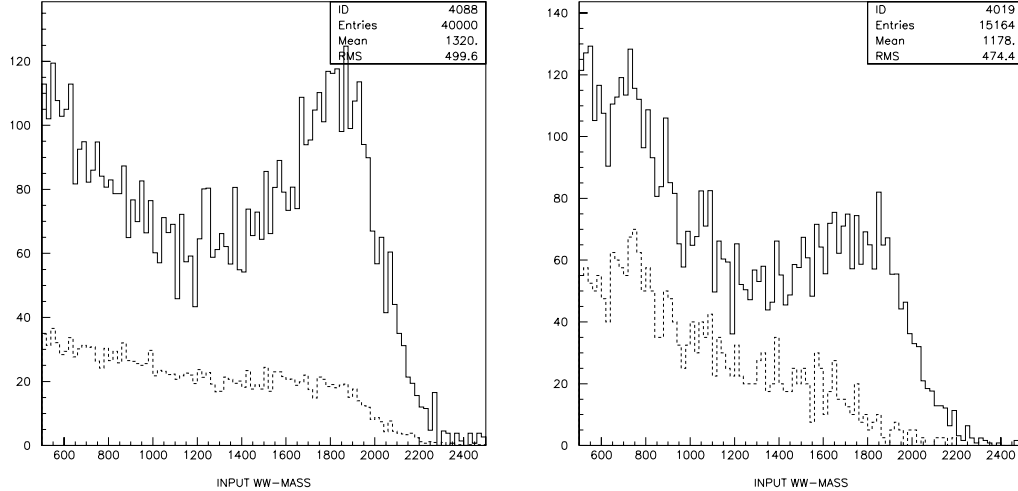


FIG. 12: Mass spectrum for  $WW$  scattering and  $WZ$  and  $ZZ$  scattering backgrounds for  $\alpha_5 = -0.002, \alpha_0 = 0.0$ , before detector (left) and after detector smearing and addition of  $\gamma\gamma$  background (right) [37].

## VI. $W^+W^-$ SCATTERING

In the scenario that no Higgs boson with large gauge boson couplings and a mass less than about 700 GeV is found, then the  $W^\pm, Z$  bosons are expected to develop strong interactions at scales of order 1-2 TeV. Generally one expects an excess of events above Standard Model expectation, and, possibly, resonance formation.

The reaction  $e^+e^- \rightarrow \nu\bar{\nu}W_L^+W_L^-$  at 3 TeV was studied using two approaches. The Chirally-Coupled Vector Model [34] for  $W_LW_L$  scattering describes the low-energy behaviour of a technicolor-type model with a Techni- $\rho$  vector resonance  $V(\text{spin-1, isospin-1 vector resonance})$ . The mass of the resonance can be chosen and the cases  $M \sim 1.5, 2.0$  and  $2.5$  TeV were studied.

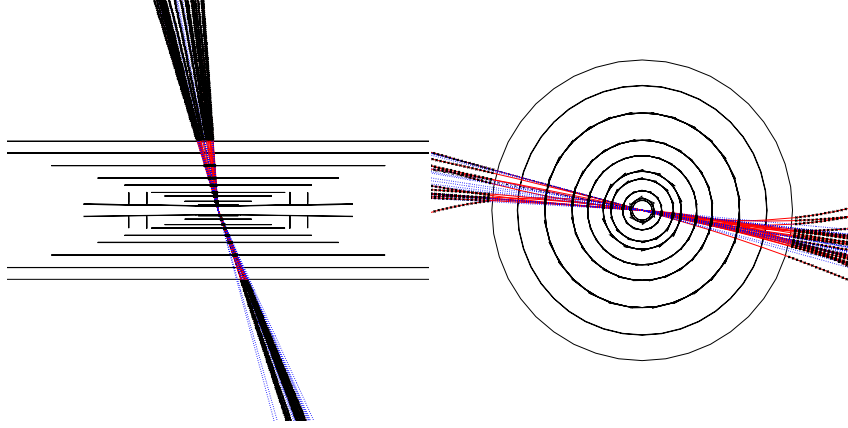


FIG. 13: Two views of an event in the central detector, of the type  $e^+e^- \rightarrow WW\nu\nu \rightarrow 4 \text{ jets } \nu\nu$ , from a resonance with  $M_{WW} = 2 \text{ TeV}$  [37].

TABLE VIII: Cross sections for vector resonances in  $WW$  scattering, with cuts as given in the text

| $\sqrt{s}$            | M=1.5 TeV                 | M=2.0 TeV                 | M=2.5 TeV                  |
|-----------------------|---------------------------|---------------------------|----------------------------|
| 3 TeV                 | $\Gamma = 35 \text{ GeV}$ | $\Gamma = 85 \text{ GeV}$ | $\Gamma = 250 \text{ GeV}$ |
| $\sigma \text{ (fb)}$ | 4.5                       | 4.3                       | 4.0                        |

In a second approach, the prescription given in [35, 36] using the electroweak Chiral Lagrangian (EHChL) Formalism is applied. The Higgs terms in the SM Lagrangian are replaced by terms in the next order of the Chiral expansion. Unitarity corrections are important for energies larger than 1 TeV. Here the Pade (Inverse Amplitude) protocol has been used. The parameters  $\alpha_4$  and  $\alpha_5$  quantify our ignorance of the new physics. High mass vector resonances will be produced in  $WW$  and  $WZ$  scattering for certain combinations of  $\alpha_4$  and  $\alpha_5$ .

The total cross section for  $WW \rightarrow WW$  scattering with the values  $\alpha_4 = 0.0$  and  $\alpha_5 = -0.002$ , amounts to 12 fb in  $e^+e^-$  collisions at 3 TeV, and is measurable at a high luminosity LC. With these parameters a broad resonance is produced at 2 TeV in the  $WW$  invariant mass, as shown in Fig. 12. A detector study is performed for this scenario, implemented in the PYTHIA generator [35]. Events are selected with the following cuts:  $p_T^W > 150 \text{ GeV}$ ,  $|\cos \Theta^W| < 0.8$ ;  $M_W > 500 \text{ GeV}$ ;  $p_T^{WW} < 300 \text{ GeV}$ ; and  $(200 < M_{rec} < 1500 \text{ GeV})$ , with  $M_{rec}$  the recoil mass. Cross sections including these cuts for different masses and widths are calculated with the program of [34] and are given in Table VIII.

The big advantage of an  $e^+e^-$  collider is the clean final state, which allows for the use of the hadronic decay modes of the  $W$ 's in selecting and reconstructing events. Four jets are produced in the decay of the two  $W$ 's. However, due to the boost from the decay of the heavy resonance, the two jets of a  $W$  are very collimated, and close to each other as shown in Fig. 13. With the present assumptions on the energy flow in SIMDET, the resolution to reconstruct the  $W, Z$  mass is about 7%.

A full spectrum which contains contributions from all the channels  $ZZ \rightarrow ZZ, ZZ \rightarrow WW, ZW \rightarrow ZW, WW \rightarrow ZZ$  and  $WW \rightarrow WW$  is shown for  $1.6 \text{ ab}^{-1}$  in Fig. 12, before and after detector smearing with parameters  $\alpha_5 = -0.002, \alpha_0 = 0.0$  [37].

Clearly heavy resonances in  $WW$  scattering can be detected at CLIC. The signal is not heavily distorted by detector resolution and background. Depending on the mass and width of the signal, about a 1000 events/year could be fully reconstructed in the 4-jet mode at CLIC. Good energy and track reconstruction will be important to remove backgrounds and reconstruct the resonance parameters (and hence the underlying model parameters) accurately.

## VII. EXTRA DIMENSIONS

For the past few years the phenomenology of large extra dimensions has been explored at the TeV scale. These theories aim to solve the hierarchy problem by bringing the gravity scale closer to the electroweak scale. (If you cannot get to the Planck scale, try to bring the Planck scale to you.) The hidden extra dimensions can

dramatically change the strength of gravity, and bring the Planck scale down to the TeV region.

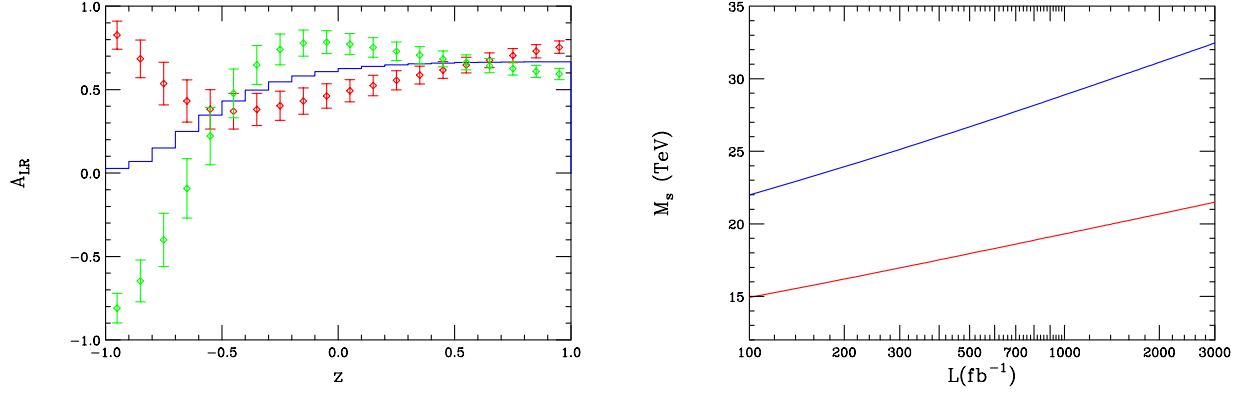


FIG. 14: (Left) Deviations in the cross section for  $A_{LR}$  for  $b$ -quarks at  $\sqrt{s}=5$  TeV for  $M_s = 15$  TeV in the ADD model for an integrated luminosity of  $1 \text{ ab}^{-1}$ . The SM is represented by the histogram while the red and green data points show the ADD predictions with  $\lambda = \pm 1$ . In both plots  $z = \cos \theta$ . (Right) Search reach for the ADD model scale  $M_s$  at CLIC as a function of the integrated luminosity from the set of processes  $e^+e^- \rightarrow f\bar{f}$  assuming  $\sqrt{s} = 3$ (red) or 5(blue) TeV. Here  $f = \mu, \tau, b, c, t$ , etc [38].

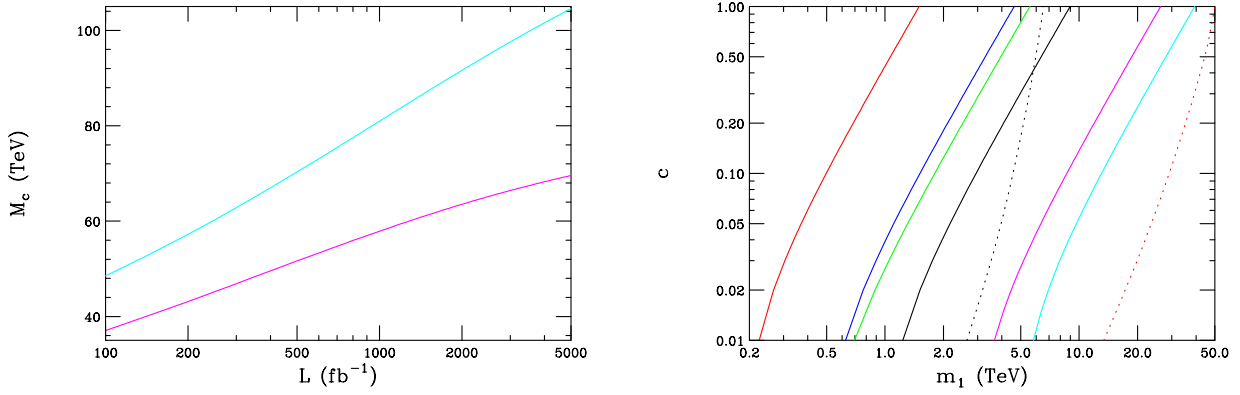


FIG. 15: (Left) Corresponding reach for the compactification scale of the KK gauge bosons in the case of one extra dimension and all fermions localized at the same orbifold fixed point. (Right) Indirect constraints from  $e^+e^-$  colliders on the RS model parameter space with  $c = k/\overline{M}_{Pl}$ ; the excluded region is to the left of the curves. From left to right the solid curves correspond to bounds from LEP II, a 500 GeV LC with 75 or 500  $fb^{-1}$  luminosity, a TeV machine with 200  $fb^{-1}$ , and a 3 or 5 TeV CLIC with  $1 \text{ ab}^{-1}$ . The dotted lines are the corresponding LHC ( $100 \text{ fb}^{-1}$ ) and  $\sqrt{s} = 175$  TeV VLHC( $200 \text{ fb}^{-1}$ ) direct search reaches [38].

Extra dimension signatures at future colliders, particularly at CLIC, have been discussed in detail in [38]. There is a wide variety of models which can be basically classified in three groups. (i) The first model is the so called large extra dimensions scenario of Arkani-Hamed, Dvali and Dimopoulos(ADD)[39]. This model predicts the emission and exchange of large Kaluza-Klein(KK) towers of gravitons that are finely-spaced in mass. The emitted gravitons appear as missing energy while the KK tower exchange leads to contact interaction-like dimension-8 operators. (ii) A second possibility are models where the extra dimensions are of TeV scale in size. In these scenarios there are KK excitations of the SM gauge (and possibly other SM) fields with masses of order a TeV which can appear as resonances at colliders [40]. (iii) A last class of models are those with warped extra dimensions, such as the Randall-Sundrum Model(RS)[41], which predict graviton resonances with both weak scale masses and couplings to matter.

High energy  $e^+e^-$  colliders in the multi-TeV range with sufficient luminosity, such as CLIC, will be able to both directly and indirectly search for and/or make detailed studies of models in all three classes.

Figs. 14 and 15 show the reach for indirect measurements in the channel  $e^+e^- \rightarrow f\bar{f}$  for a multi-TeV collider, from [38]. The convention used in [42] is adopted, expressing the contributions to spin-2 exchanges in terms of the scale  $M_s$  and a sign  $\lambda$ . Fig. 14a shows how such deviations from the SM can manifest themselves at a 5 TeV

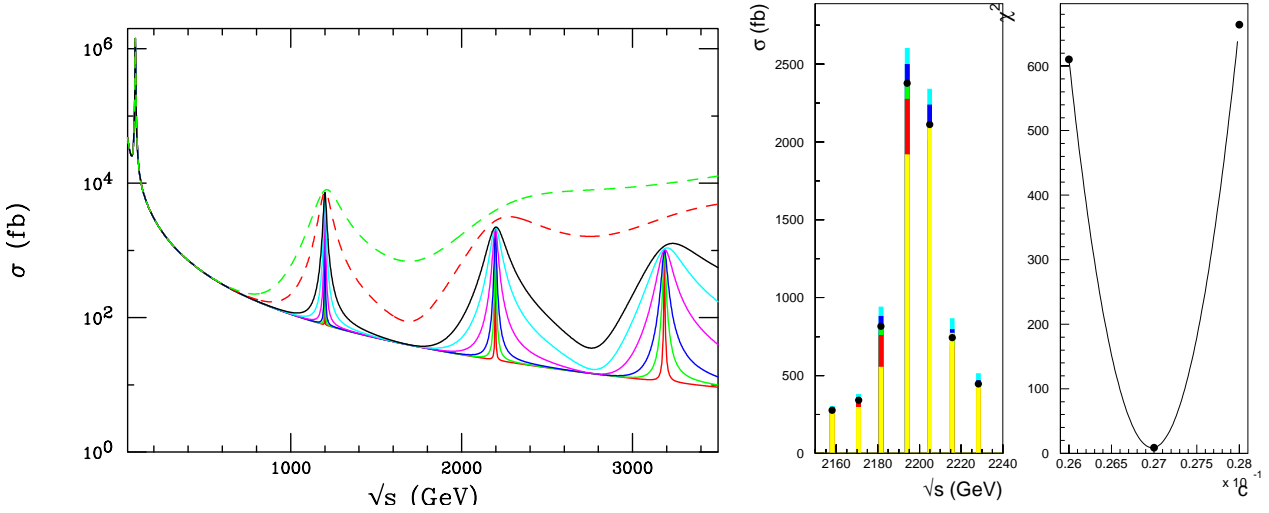


FIG. 16: (Left) KK graviton excitations in the RS model produced in the process  $e^+e^- \rightarrow \mu^+\mu^-$ . From the most narrow to widest resonances the curves are for  $c$  in the range 0.01 to 0.2. (Right) Scan of the resonance (7 points) and  $\chi^2$  fit to the measured spectrum for models with different values for  $c$  [38, 43].

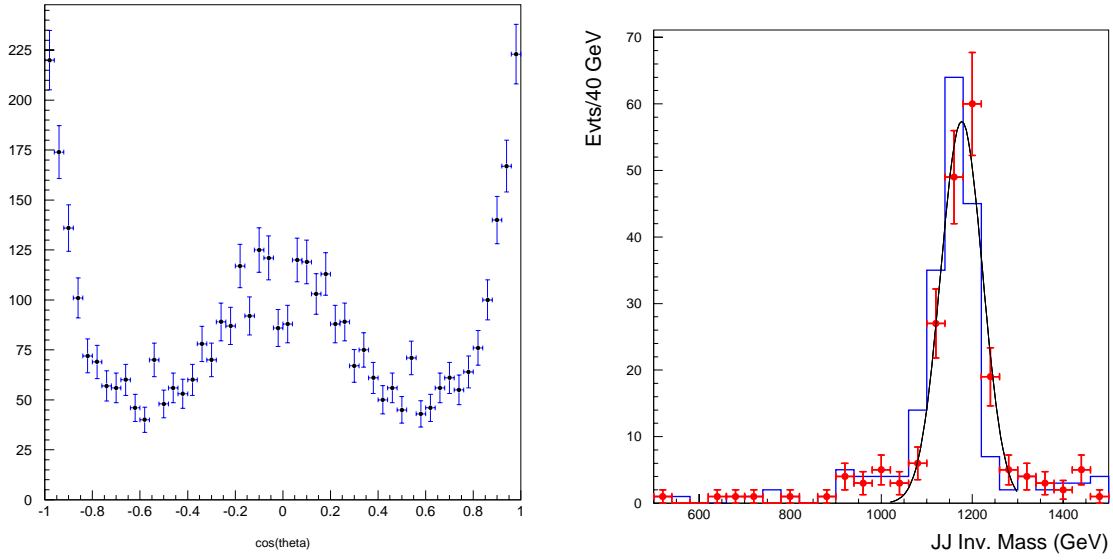


FIG. 17: (Left) Angular distribution of produced muons from decay of a graviton. (Right) Reconstructed mass distribution of the  $G_1$  graviton decaying into two jets [43].

CLIC in case  $M_s = 15$  TeV, for the two signs of  $\lambda$ . For the evaluation of the search reach several fermion final states have been combined. The results on the search reach versus the available luminosity are shown in Fig. 14b. Fig. 15 shows search reaches for examples of the other two model classes (see [38]). In summary a multi-TeV collider has a sensitivity to reach up to 20-80 TeV, depending on the model, from precision measurements.

Direct measurements can be made in the RS and TeV scale extra dimension models. In the Randall-Sundrum model [41] TeV scale graviton resonances are expected in many channels. In its simplest version, with two branes and one extra dimension, and all of the SM fields remaining on the brane, the model has two fundamental parameters: the mass of the first resonance and the parameter  $c = k/M_{Pl}$  which should be less than but not too far away from unity. This parameter controls the effective coupling strength of the graviton and thus the width of the resonances. A spectrum for  $e^+e^- \rightarrow \mu^+\mu^-$  is given in Fig. 16a. Clearly the cross sections are huge and a putative signal cannot be missed by a LC with sufficient CMS energy. This LC will be like a KK

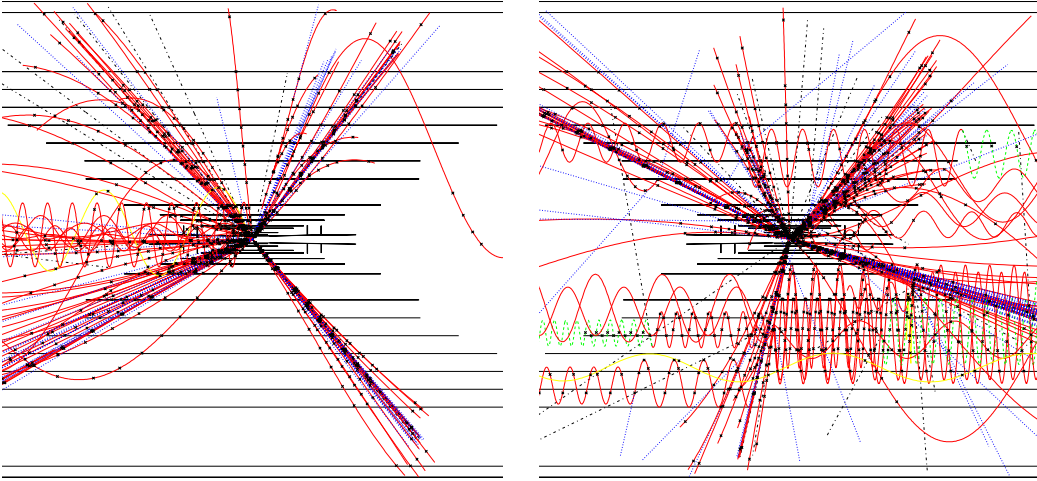


FIG. 18: Graviton resonance  $G_3$  decaying into  $G_1 G_1 \rightarrow 4$  jets [43].

resonance factory, up to the kinematic limit, and can be used to measure the properties ( $M, c$ , branching ratios) and quantum numbers (spin) of the KK resonances.

The signal for high energy resonance ( $G_3$  at 3200 GeV) has been selected via either two muons or two  $\gamma$ 's with  $E > 1200$  GeV and  $|\cos \theta| < 0.97$ . The background from overlaid two photon events is typically below 120 mrad, thus mostly outside the signal region. A scan similar to the one for the  $Z$  at LEP, folded with the CLIC luminosity spectrum, was made for an integrated luminosity of  $1 \text{ ab}^{-1}$ , and results in a precision to determine  $c$  to 0.2% and  $M$  to better than 0.1% [43]. An example of such a scan is shown in Fig. 16b.

The graviton is a spin-two object. Fig. 17 shows the decay angle of the fermions from  $G \rightarrow \mu\mu$  for the lightest graviton, for  $1 \text{ ab}^{-1}$  of data, using signal events and including machine background. The spin-two nature of the resonance is clearly visible. Another property of these gravitons is  $BR(G \rightarrow \gamma\gamma)/BR(G \rightarrow \mu\mu) = 2$ . These events can be easily selected by cuts on isolated muons and photons, even in the presence of machine background [43]. Hence the ratio  $BR(G \rightarrow \gamma\gamma)/BR(G \rightarrow \mu\mu)$  can be measured with a precision better than 1%.

Furthermore, if the energy of the collider is large enough to see the first three graviton resonances, there is the intriguing opportunity to measure the graviton self coupling in  $G \rightarrow GG$  decay ( $\sim 15\%$  of decays) [44]. The dominant decay mode is  $G \rightarrow \text{gluon-gluon}$  into jets. A few examples of events decaying into 4 jets are shown in Fig. 18. Fig. 17 shows the reconstruction of the  $G_1$  mass from 2 jets from  $G_3 \rightarrow G_1 G_1$  decay. The histogram contains no background, while the points contain 10 bunch crossings of  $\gamma\gamma$  background overlaid. The  $G_1$  graviton signal can be easily reconstructed in the decay of the  $G_3$  graviton.

If KK resonances are produced in the TeV region, then CLIC can be used to precisely determine the shape, mass, spin, and branching ratios of the objects. With such information the objects can be unambiguously identified as gravitons.

## VIII. NON COMMUTATIVE THEORIES

Recently theoretical results have demonstrated that non-commutative (NC) geometries naturally appear within the context of string/M theories [45]. In such theories the conventional space-time coordinates, which are represented by operators, no longer commute, due to a preferred direction in space, and Lorentz invariance is violated. The effect can be parameterized by a scale  $\Lambda_{NC}$ , which characterizes the threshold at which NC effects become important. The most likely value of  $\Lambda_{NC}$  is close to the Planck scale, and with the recent ideas of extra dimensions in which the Planck scale might be as low as a few TeV, there exists the possibility of observing such stringy effects at colliders.

A consequence of a NC quantum field theory is that QED takes on a non-abelian nature due to new 3 and 4-point photon couplings. This will have striking effects on Bhabha and Møller scattering, and on the

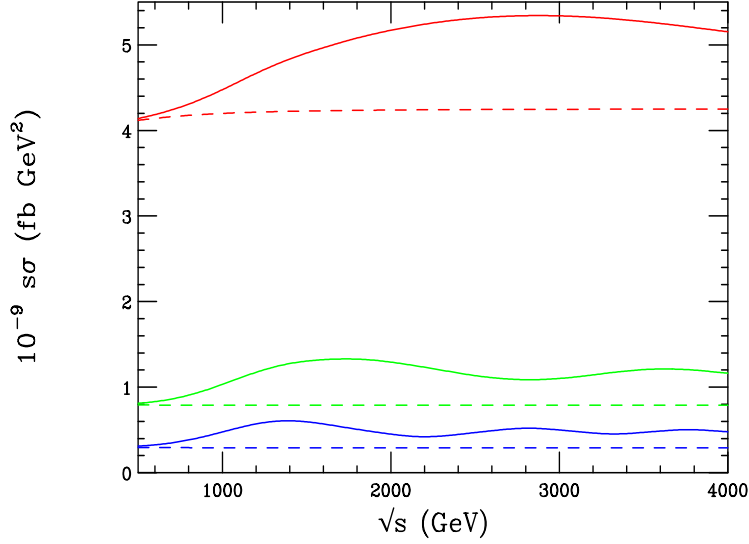


FIG. 19: The scaled cross section for Bhabha scattering including  $\cos\theta$  cuts on the scattered electrons: (from top to bottom)  $\cos\theta < 0.9/0.7/0.5$ , for  $\Lambda_{NC} = 500$  GeV. Dashed curves are the SM production [45].

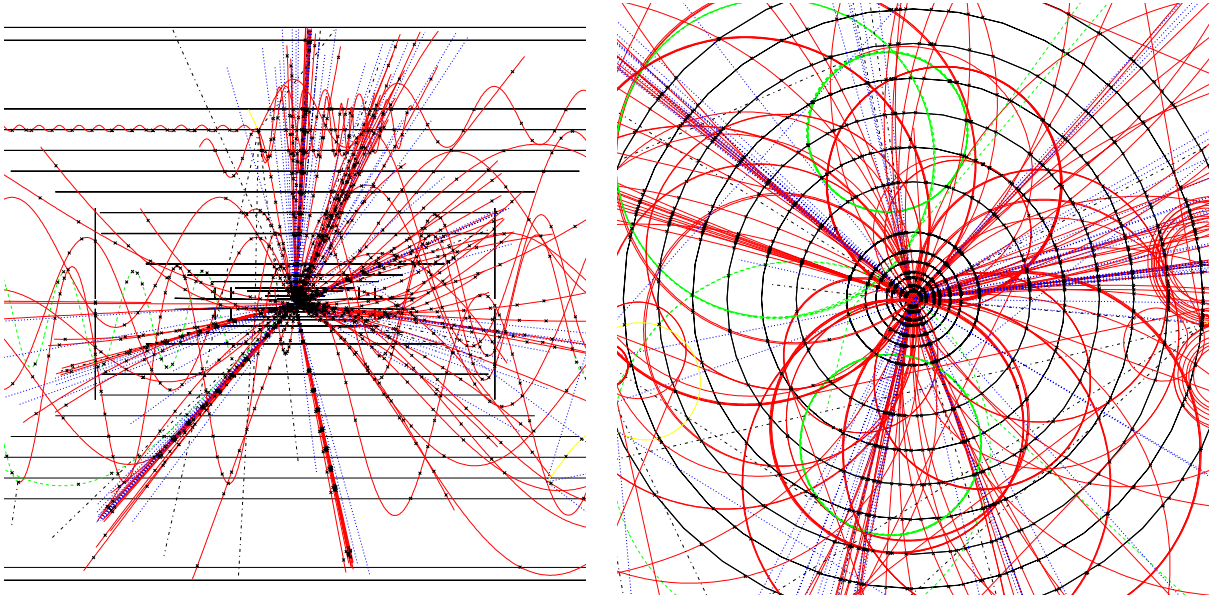


FIG. 20: Black hole production in the CLIC detector.

reaction  $\gamma\gamma \rightarrow \gamma\gamma$ . The non-abelian nature of QED can be tested by looking for unexpected structure in kinematic variable distributions caused by  $s$ - and  $t$ -channel interference. For example, Fig. 19 shows the energy dependence of the scaled Bhabha cross section as function of the CMS energy, for different  $\cos\theta$  selections for the scattered electrons. The variation results from the momentum dependent phase factors present at the QED vertices. The effects can be large and modulations of order 20%-30% are expected for this choice of model parameters [45].

The sensitivity to  $\Lambda_{NC}$  for a 3 and 5 TeV collider has been studied in detail in [45]. For the reaction  $e^+e^- \rightarrow \gamma\gamma$  the search reach (95%) for  $1 \text{ ab}^{-1}$  is  $\Lambda_{NC} \sim 2.5 - 3.5$  (3 TeV) and  $3.8 - 5.0$  (5 TeV). For the reaction  $e^+e^- \rightarrow e^+e^-$  the search reach (95%) for  $1 \text{ ab}^{-1}$  corresponds to  $\Lambda_{NC} \sim 4.5 - 5.0$  (3 TeV) and  $6.6 - 7.2$  (5 TeV), and shows a larger sensitivity.

Hence NC effects, if present at the TeV scale, will produce large characteristic effects in the data at a multi-TeV collider.

## IX. BLACK HOLE PRODUCTION

Another idea to emerge from all the recent work on extra dimensions is the laboratory production of black holes. If the fundamental Planck scale is in the TeV range then a natural consequence would be the possibility of black hole (BH) production in the multi-TeV range, above the Planck scale. The cross section is expected to be very large:  $\sigma = \pi R_s^2 \sim 1 \text{ TeV}^{-2} \sim O(100) \text{ pb}$ , where  $R_s$  is the Schwarzschild Radius. If  $\sqrt{s}_{e^+e^-} > M_{BH} > M_{\text{Planck}}$  then the collider becomes a black hole factory. The lifetime of such a black hole is of order  $\sim 10^{-25} - 10^{-27}$  sec, and hence the black hole will evaporate before it could possibly ‘attack’ any detector material. Hence these mini black holes are not dangerous for mankind. Furthermore, if black hole production can take place in multi-TeV  $e^+e^-$  collisions, then cosmic ray neutrinos with energies in excess of  $10^3 \text{ TeV}$  have been producing mini black holes in collisions with earth’s atmosphere throughout its history [46].

The decay of a black hole can be very complex and involve several stages [47, 48]. If the dominating mode is Hawking radiation then all particles (quarks, gluons, gauge bosons, leptons) are expected to be produced democratically, with e.g. a ratio 1/5 between leptonic and hadronic activity. The multiplicity is expected to be large. The production and decay process have been included in the PYTHIA generator[48]. Fig. 20 shows two black hole events produced in a detector at CLIC, leading to spectacular multi-jet and lepton/photon signals. If this scenario is realized in Nature black holes will be produced at high rates at the LHC. CLIC can be very instrumental in providing precise measurements. For example, it could be used to test Hawking radiation and extract the number of underlying extra dimensions.

The large production cross section, low backgrounds and little missing energy would make BH production and decay a perfect laboratory to study strings and quantum gravity.

Besides the black holes other novel ideas include:

- String quantum gravity effects in  $e^+e^- \rightarrow e^+e^-$  and  $\gamma\gamma$  [49]
- Brane fluctuation modes (Nylons?) [50]
- Split Fermions in Extra Dimension [51]
- Extra Dimensions & Two Supersymmetries [52]

If any of these scenarios occurs in Nature a multi-TeV  $e^+e^-$  collider promises to be extremely instrumental and useful to explore this new physics domain.

TABLE IX: Measurements at CLIC (5 TeV / 1  $\text{ab}^{-1}$ , unless otherwise stated).

|                                   |   |
|-----------------------------------|---|
| Higgs (Light)                     | $g_{HHH}$ to $\sim 7 - 10\%$ (5 $\text{ab}^{-1}$ / 3 TeV)     |
| Higgs (Light)                     | $g_{H\mu\mu}$ to $\sim 4 - 10\%$ (5 $\text{ab}^{-1}$ / 3 TeV) |
| Higgs (Heavy)                     | 2.0 TeV ( $e^+e^-$ ) 3.5 TeV ( $\gamma\gamma$ )               |
| squarks                           | 2.5 TeV   |
| sleptons                          | 2.5 TeV   |
| Z' (direct)                       | 5 TeV   |
| Z' (indirect)                     | 20-30 TeV   |
| $l^*, q^*$                        | 5 TeV   |
| TGC (95%): $\Delta\lambda_\gamma$ | 0.00008   |
| TGC (95%): $\Delta\kappa_\gamma$  | 0.00005   |
| $\Lambda$ compos.                 | 400 TeV   |
| $W_L W_L$                         | > 5 TeV   |
| ED (ADD)                          | 30 TeV ( $e^+e^-$ )<br>55 TeV ( $\gamma\gamma$ )              |
| ED (RS)                           | 18 TeV ( $c=0.2$ )  |
| ED ( $\text{TeV}^{-1}$ )          | 80 TeV  |
| Resonances                        | $\delta M/M, \delta\Gamma/\Gamma \sim 10^{-3}$                |
| Black Holes                       | 5 TeV   |

## X. SUMMARY

Linear  $e^+e^-$  colliders operating in the multi-TeV energy range are likely to be based on the CLIC two-beam acceleration concept. To achieve a large luminosity, such an accelerator would need to operate in the high beamstrahlung region, rendering experimentation at such a collider more challenging. Studies so far indicate that this is not a substantial handicap, and the precision physics expected from an  $e^+e^-$  collider will be possible.

The two-beam accelerator technology is not yet available today for use at a large scale collider. R&D on this technology will continue until 2006 at least, after which – if no bad surprises emerge – one can plan for a full technical design of such a collider.

From the physics program side, a multi-TeV collider has a large potential to push back the high energy horizon further, up to scales of 1000 TeV, where – if the Higgs is light – new physics can no longer hide from experiment. If no new scale is found by then we have to revise our understanding of Nature.

A multi-TeV collider with high luminosity can be used for precision measurements in the Higgs sector. It can precisely measure the masses and couplings of heavy sparticles, thereby completing the SUSY spectrum. If extra dimensions or even black holes pop up in the multi-TeV range, such a collider will be a precision instrument to study quantum gravity in the laboratory.

The physics reach, as envisioned today, for a multi-TeV collider is summarized in Table IX. In short a collider with  $\sqrt{s} \simeq 3\text{--}5$  TeV is expected to break new grounds, beyond the LHC and a TeV class LC.

## Acknowledgments

We are grateful to the participants of the Snowmass E3-S2 subgroup on multi-TeV  $e^+e^-$  colliders, and to the CLIC physics study group, in particular T. Rizzo, J. Hewett, M. Battaglia, and D. Schulte.

- 
- [1] *The Superconducting Electron-Positron Linear Collider with an Integrated X-Ray Laser Laboratory Technical Design Report*, DESY 2001-011.
  - [2] *2001 Report on the Next Linear Collider*, SLAC-R-571.
  - [3] JLC-1, JLC Group, S Matsumoto et al., KEK report 92-16.
  - [4] P. Burrows and R. Patterson, *LC Expandability and Upgradability*, these proceedings..
  - [5] M. Battaglia, hep-ph/0103338.
  - [6] The CLIC Study Team, *A 3 TeV  $e^+e^-$  Linear Collider Based on CLIC Technology*, CERN 2000-008.
  - [7] H.H. Braun et al., Proc. of 18th International Conference on High Energy Accelerators (HEACC'2001), 26-30 March 2001, Tsukuba, Japan, and CLIC Note 473; see also <http://geschonk.home.cern.ch/geschonk/>
  - [8] R. Corsini et al., CERN/PS 2001-030 (AE), and 2001 Particle Accelerator Conference (PAC'2001), Chicago, Illinois, USA, June 18-22, 2001
  - [9] D. Asner et al., hep-ex/0111056
  - [10] V. Telnov, *Photon Colliders at Multi-TeV Energies*, these proceedings.
  - [11] R. Assmann and F. Zimmerman, *Polarization at CLIC*, these proceedings.
  - [12] G. Guignard, *The CLIC Study*, these proceedings.
  - [13] D. Schulte, *Machine-detector Interface at CLIC*, these proceedings  
D. Schulte, CERN-PS-99-066.
  - [14] R. Settles, *Detector Requirements at Multi-TeV LC*, these proceedings.
  - [15] M. Battaglia, in Proceedings of the LCWS2000 workshop, p831.
  - [16] M. Pohl and H.J. Schreiber, *SIMDET - A parametric Monte Carlo for a TESLA detector*, DESY 99-030.
  - [17] M. Battaglia, adaption of the DELPHI PVEC package.
  - [18] M. Battaglia, E. Boos, and W. Yao, *Studying the Higgs Potential at the Linear Collider*, hep-ph/0111276 .
  - [19] M. Battaglia, A. De Roeck, *Determination of the Muon Yukawa Coupling at High Energy  $e^+e^-$  Linear Colliders*, these proceedings, hep-ph/0111307.
  - [20] J. F. Gunion (1997), hep-ph/9703203.
  - [21] T. Plehn and D. Rainwater, Phys. Lett. **B520**, 108 (2001), hep-ph/017180.
  - [22] Marco Battaglia et al., hep-ph/0106204.
  - [23] M. Battaglia, A. Kiiskinen and A. Ferrari, *Study of Charged Higgs Bosons*, these proceedings, hep-ex/0112015.
  - [24] G. Blair, W. Porod, P.M. Zerwas Phys. Rev. **D63** (2001) 017703, hep-ph/0007107.
  - [25] G. Moortgat-Pick, *Physics Opportunities with Polarized  $e^-$  and  $e^+$  Beams at a Linear Collider*, these proceedings.
  - [26] G. Wilson in Proceedings of the LCWS2000 workshop, p485.
  - [27] M. Battaglia, Private communication.
  - [28] M. Klasen, Talk at the Workshop on gamma-gamma colliders, Chicago 2001.
  - [29] A. Ferrari, *Study of Majorana Neutrinos at CLIC*, these proceedings.

- [30] M. Battaglia, S. Riemann, S. De Curtis and D. Dominici, *Probing New Scales at  $e+e-$  Linear Collider*, these proceedings;  
Battaglia et al., hep-ph/0101114.
- [31] E. Eichten, K Lane and M. Peskin, Phys. Rev. Lett **50** (1983) 811; H. Kroha, Phys. Rev. **D46** (1992) 58.
- [32] T. Hambye and K. Riesselmann, Phys. Rev. **D55** (1997) 7255, hep-ph/9708416.
- [33] T. Barklow, private communication.
- [34] D. Barger et al., Phys Rev. **D52** (1995) 3815, Phys Rev. **D55** (1997) 142.
- [35] M. Butterworth, B.E. Cox and J.R. Forshaw, in preparation.
- [36] A. Dobado et al., Phys Rev **D62** (2000) 05501.
- [37] A. De Roeck, *WW Scattering at CLIC*, these proceedings.
- [38] T. Rizzo, hep-ph/0108235.
- [39] N. Arkani-Hamed, S. Dimopoulos, and G. Dvali, Phys. Lett. **B429**, 263 (1998), and Phys. Rev. **D59**, 086004 (1999);  
I. Antoniadis, N. Arkani-Hamed, S. Dimopoulos, and G. Dvali, Phys. Lett. **B436**, 257 (1998).
- [40] See, for example, I. Antoniadis, Phys. Lett. **B246**, 377 (1990); I. Antoniadis, C. Munoz and M. Quiros, Nucl. Phys. **B397**, 515 (1993); I. Antoniadis and K. Benalki, Phys. Lett. **B326**, 69 (1994) and Int. J. Mod. Phys. **A15**, 4237 (2000); I. Antoniadis, K. Benalki and M. Quiros, Phys. Lett. **B331**, 313 (1994).
- [41] L. Randall and R. Sundrum, Phys. Rev. Lett. **83**, 3370 (1999).
- [42] For an introduction to ADD phenomenology, see G.F. Giudice, R. Rattazzi and J.D. Wells, Nucl. Phys. **B544**, 3 (1999); T. Han, J.D. Lykken and R. Zhang, Phys. Rev. **D59**, 105006 (1999), E.A. Mirabelli, M. Perelstein and M.E. Peskin, Phys. Rev. Lett. **82**, 2236 (1999); J.L. Hewett, Phys. Rev. Lett. **82**, 4765 (1999); T.G. Rizzo, Phys. Rev. **D60**, 115010 (1999).
- [43] M. Battaglia, A. De Roeck and T. Rizzo, *Graviton Production at CLIC*, these proceedings, hep-ph/0112169.
- [44] H. Davoudiasl and T. Rizzo, hep-ph/0104199.
- [45] J. Hewett, F. Petriello, and T. Rizzo, hep-ph/0010354.
- [46] J. L. Feng and A. D. Shapere, hep-ph/0109106.
- [47] S. Thomas, hep-ph/0106219.
- [48] S Dimopoulos and G. Landsberg, Phys. Rev Lett. **87** 161602 (2001).
- [49] S. Cullen, M. Perelstein, M. E. Peskin, Phys.Rev. **D62** (2000) 055012, hep-ph/0001166
- [50] J. Lykken, talk at LCWS2000.
- [51] N. Arkani-Hamed, Y. Grossman, M. Schmaltz, Phys. Rev. **D61** (2000) 115004, hep-ph/9909411.
- [52] R. Barbieri, L. J. Hall, Y. Nomura, Phys. Rev. **D63** (2001) 105007, hep-ph/0011311.